Complexes of Trivalent Metal Ions with Potentially Heptadentate N_4O_3 Schiff Base and Amine Phenol Ligands of Varying Rigidity†

Li-Wei Yang, Shuang Liu,[1] Ernest Wong, Steven J. Rettig, and Chris Orvig*

Department of Chemistry, University of British Columbia, 2036 Main Mall, Vancouver, British Columbia V6T 1Z1, Canada

Received May 10, 1994[⊗]

The synthesis and characterization of several potentially heptadentate N_4O_3 Schiff bases and amine phenols, as well as a series of their mononuclear and dinuclear complexes with indium and the lanthanides are reported. Schiff bases containing imidazolidine rings were the products of the known condensation reaction of triethylenetetramine with 3 equiv of 5-substituted salicylaldehydes to form H_3api (5-H-substituent), H_3Clapi (5-Cl-substituent), or H_3Brapi (5-Br-substituent); KBH_4 reduction of these Schiff bases gave the appropriate isomeric N_4O_3 amine phenols H_3(1,2,4-btt) and H_3(1,1,4-btt), as well as an acetone adduct, H_3(1,2,4-ahi). The Schiff bases reacted with 1 equiv of a lanthanide (Ln^{3+}) nitrate to produce mononuclear nine-coordinated [Ln(H_3Xapi)$(NO_3)_3$] complex wherein the ligand adopts a tridentate capping coordination mode, whereas the amine phenols formed mononuclear seven-coordinate complexes with the lanthanides and indium; homodinuclear complexes $[LnL]_2$ were also obtained with the Schiff bases. The X-ray structures of the Schiff bases H_3api and H_3Clapi, the mononuclear amine phenol complexes Yb(1,2,4-btt)·0.5CH_3OH and In(1,1,4-btt), and the homodinuclear Schiff base complex $[La(Brapi)]_2$·2$CHCl_3$ have been determined. Crystals of H_3api ($C_{27}H_{30}N_4O_3$) are monoclinic, space group $P2_1/a$, a = 19.281(2) Å, b = 5.774(3) Å, c = 21.999(2) Å, β = 97.85(1)°, Z = 4; those of H_3Clapi ($C_{27}H_{27}Cl_3N_4O_3$) are orthorhombic, $Pnma$, a = 11.398(4) Å, b = 21.486(3) Å, c = 10.942(4) Å, Z = 4; those of $[La(Brapi)]_2$·2$CHCl_3$ ($C_{56}H_{50}Br_6Cl_6La_2N_8O_6$) are monoclinic, space group $C2/c$, a = 22.336(1) Å, b = 14.770(2) Å, c = 22.647(2) Å, β = 116.855(5)°, Z = 4; those of Yb(1,2,4-btt)·0.5CH_3OH ($C_{27.5}H_{35}N_4O_{3.5}Yb$) are monoclinic, $P2_1/n$, a = 12.798(2) Å, b = 19.671(6) Å, c = 21.129(2) Å, β = 91.895(9)°, Z = 8; and those of In(1,1,4-btt) ($C_{27}H_{33}InN_4O_3$) are triclinic, space group $P\bar{1}$, a = 12.771(3) Å, b = 18.994(4) Å, c = 11.450(2) Å, α = 105.71(1)°, β = 99.73(1)°, γ = 89.21(2)°, Z = 4. The structures were solved by direct (organic compounds and La complex) or Patterson (Yb and In complexes) methods and were refined by full-matrix least-squares procedures to R = 0.034, 0.035, 0.042, 0.031, and 0.029 for 2386, 1444, 2800, 7570, and 8682 reflections with $I \geq 3\sigma(I)$, respectively. Both amine phenol complexes Yb(1,2,4-btt) and In(1,1,4-btt) have pentagonal bipyramidal coordination geometry around the metal ions, which are each coordinated by N_4O_3 donor sets. The structure of $[La(Brapi)]_2$ reveals that the two ligands bridge the two metal ions forming an LM_2L sandwich structure. The dinuclear $[LaBrapi]_2$ has a square antiprismatic geometry around each lanthanum atom. Each La atom is coordinated by an N_4O_4 donor set, N_2O from each ligand and two bridging phenolate O atoms, one from each heptadentate ligand with a La−La separation of 4.023(1) Å. Autoconversion of the Schiff base complexes wherein the ligand is tridentate to the sandwich structure dinuclear complexes, together with the evidence of variable-temperature ^{1}H NMR of $[La(Clapi)]_2$ in DMSO-d_6, indicates that these new sandwich $[LnL]_2$ complexes are quite stable and extremely rigid.

Introduction

Metal complexes with coordination numbers of seven or higher have received sporadic attention for many years,[2,3] but complexes containing heptadentate ligands are still rare. For a variety of transition metal complexes of Schiff bases derived from the tripodal amine tris(2-aminoethyl)amine (tren) the bond between the metal ion and the apical tertiary nitrogen atom was found to be weak.[4−9] Studies of lanthanides with related tren-based Schiff bases have also been reported,[10−12] and it was noted previously[12] that when all four nitrogens of a tripodal Schiff base coordinated to a lanthanide (Yb^{3+}), the complex was highly unstable and very sensitive to moisture, metal ion-promoted hydrolysis of the imine C=N linkages being enhanced. To obviate this problem, we have recently reported several amine phenol ligands and their lanthanide complexes[13] wherein the ligands adopted either a tridentate capping or heptadentate encapsulating coordination mode (Chart 1), depending on the reaction conditions.

In order to broaden our perspective on potentially heptadentate ligands, and to explore potential lanthanide aggregation as a

* To whom correspondence should be addressed. Tel: (604) 822-4449. FAX: (604) 822-2847. Internet: orvig@chem.ubc.ca.

†Abbreviations employed (see also Scheme 1): trien = triethylenetetramine; tren = tris(2-aminoethyl)amine; H_3api = 2-(2′-hydroxyphenyl)-1,3-bis[3′-aza-4′-(2″-hydroxyphenyl)prop-4′-en-1′-yl]-1,3-imidazolidine; H_3Clapi = 2-(2′-hydroxy-5′-chlorophenyl)-1,3-bis[3′-aza-4′-(2″-hydroxy-5″-chlorophenyl)-prop-4′-en-1′-yl]-1,3-imidazolidine; H_3Brapi =2-(2′-hydroxy-5′-bromophenyl)-1,3-di[3′-aza-4′-(2″-hydroxy-5″-bromophenyl)-prop-4′-en-1′-yl]-1,3-imidazolidine; H_3(1,2,4-btt) = *N,N′,N″*-tris(2-hydroxybenzyl)-triethylenetetramine; H_3(1,1,4-btt) = *N,N,N″*-tris(2-hydroxybenzyl)triethylenetetramine; H_3(1,2,4-ahi) = 1-(2′-hydroxybenzyl)-2,2-dimethyl-3-[3′,6′-diaza-3′-(2″-hydroxybenzyl)-7′-(2″-hydroxyphenyl)-heptyl]-1,3-imidazolidine.

⊗ Abstract published in *Advance ACS Abstracts*, March 1, 1995.

(1) Natural Sciences and Engineering Research Council Postdoctoral Fellow 1991−1993.
(2) Drew, M. G. B. *Prog. Inorg. Chem.* **1977**, *23*, 67.
(3) Drew, M. G. B. *Coord. Chem. Rev.* **1977**, *24*, 179.
(4) Wilson, L. J.; Rose, N. J. *J. Am. Chem. Soc.* **1968**, *90*, 6041.
(5) Cook, D. F.; Cummins, D.; McKenzie, E. D. *J. Chem. Soc., Dalton. Trans.* **1976**, 1369.
(6) Sim, P. G.; Sinn, E. *Inorg. Chem.* **1978**, *17*, 1288.
(7) Malek, A.; Dey, G. C.; Nasreen, A.; Chowdhury, T. A.; Alyea, E. C. *Synth. React. Inorg. Met.-Org. Chem.* **1979**, *9*, 145.

0020-1669/95/1334-2164$09.00/0

Chart 1

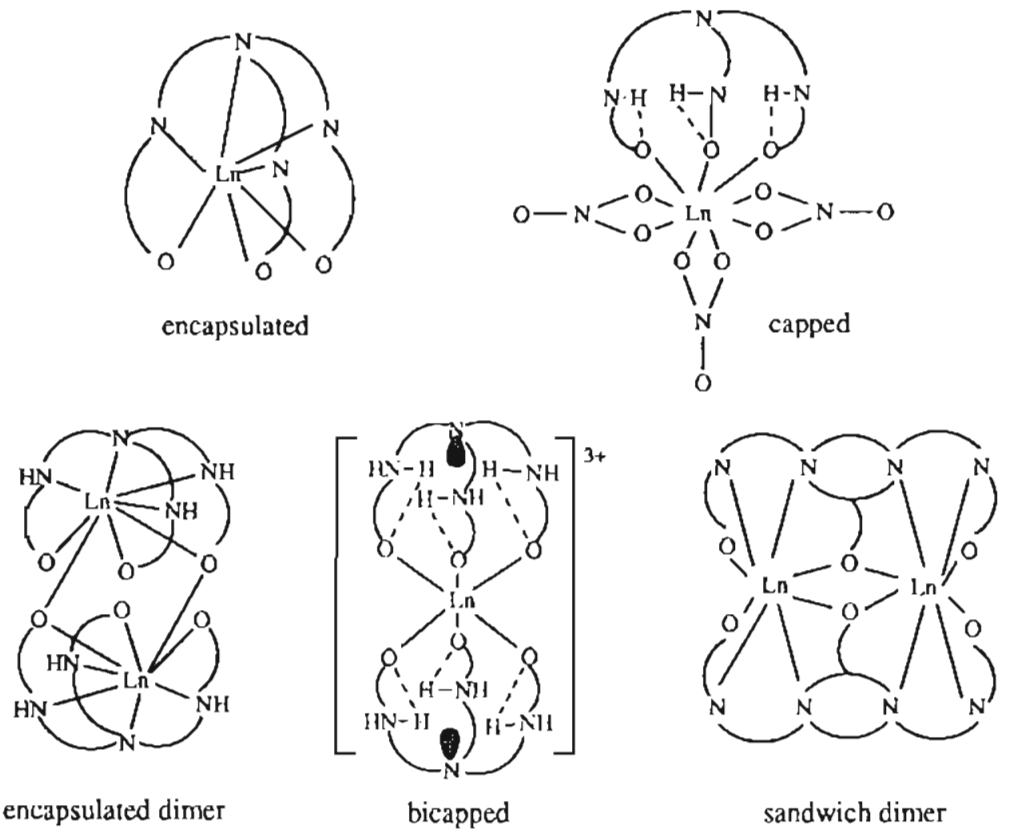

Scheme 1

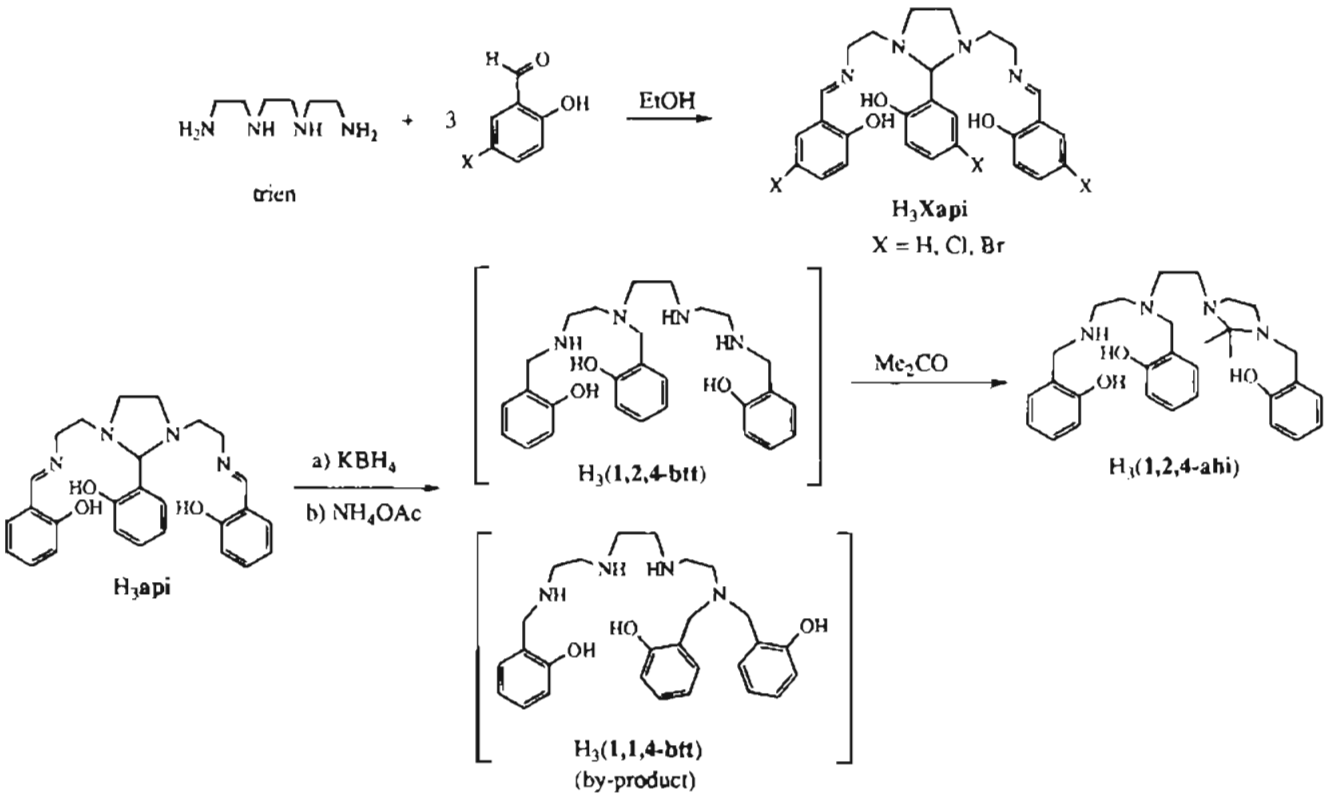

function of flexibility in the ligand, we have taken advantage of the known[13-18] imidazolidine ring formation reaction shown in Scheme 1 to prepare the N_4O_3 Schiff bases based on the H_3-Xapi framework (H_3api, H_3Clapi, H_3Brapi—see list of abbreviations and Scheme 1). These ligands are potentially heptadentate

(8) Alcock, N. W.; Cook, D. F.; McKenzie, E. D.; Worthington, J. M. *Inorg. Chim. Acta* **1980**, *38*, 107.

(9) Kirchner, R. M.; Mealli, C.; Bailey, M.; Howe, N.; Torre, L. P.; Wilson, L. J.; Andrews, L. C.; Rose, N. J.; Lingafelter, E. C. *Coord. Chem. Rev.* **1987**, *77*, 89.

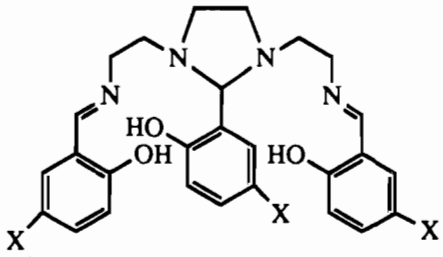

H_3Xapi X = H H_3api; X = Cl H_3Clapi; X = Br H_3Brapi

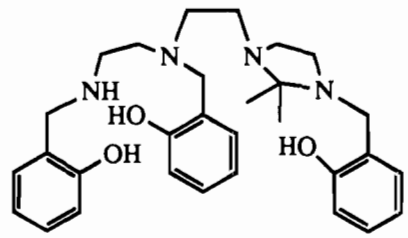

$H_3(1,2,4\text{-ahi})$

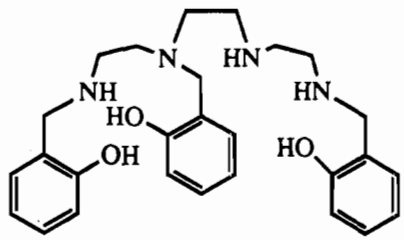

$H_3(1,2,4\text{-btt})$

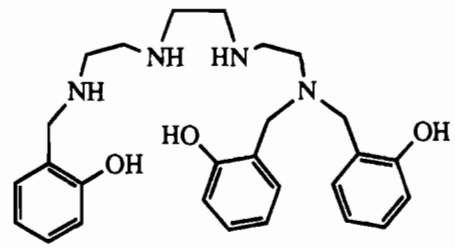

$H_3(1,1,4\text{-btt})$

but should have their chelating arms spread wide to allow for bridging of two metal ions. H_3api has been reported previously, ironically as a nuisance byproduct of a side-reaction in Schiff base formation with multidentate amines.[14-18] When H_3api is coordinated to metal ions such as Co(III), Fe(III), Mn(III), Ga(III), Al(III), Co(II), Ni(II), and Cu(II) in a 1:1 ratio,[14,15,18] it was found that one molecule of salicylaldehyde split off to decrease the steric constraints of the ligand around the metal ion and an N_4O_2 chelate formed. It was also reported that no arm was lost if a 2:1 ratio was employed for Fe(III).[17] Studies on its sulfonated analog[19] and evaluation of its methoxy-substituted analog as a potential ^{68}Ga radiopharmaceutical for myocardial imaging[18] have also been performed. In order to have a better understanding of the coordination chemistry and the steric effects of this ligand, we have characterized the lanthanide complexes of this Schiff base and its isomeric amine phenol reduction products. The complexes of chloride- and bromide-substituted Schiff bases were also examined in order to facilitate crystallization and handling.

In this paper, we present the first structurally characterized homodinuclear complex $[La(Brapi)]_2$ in which two identical ligands together form two compartments to give a sandwich LM_2L structure, and we also present the novel conversion of a complex in which a tridentate capped ligand spontaneously incorporates two lanthanide ions into the 2:2 Ln:L sandwich species, a conversion which shows that these sandwich Schiff base complexes are quite stable. Schiff base complexes have been studied extensively since it is recognized that many complexes of this type with N_xO_y donor sets may serve as models for biologically important metal-containing species; however, in studies of dinuclear complexes, the emphasis has been mainly on macrocyclic ligands, macrocycles with one open side (one-side-off or end-off compartmental ligands), or polypodal ligands.[20] Although several crystal structures of homodinuclear lanthanide complexes have been reported,[13,21-26] none of them has the sandwich structure.

Experimental Section

Materials and Methods. Hydrated lanthanide salts, triethylenetetramine hydrate (trien), potassium borohydride, salicylaldehyde, 5-chlorosalicylaldehyde, and 5-bromosalicylaldehyde were purchased from Aldrich or Alfa and were used without further purification.

Infrared spectra were recorded as KBr disks in the range 4000−400 cm^{-1} on a Perkin-Elmer PE 783 spectrometer and were referenced to polystyrene. NMR spectra (200, 400, and 500 MHz) were recorded on Bruker AC-200E ($^1H-^1H$ COSY and APT ^{13}C), Bruker WH-400 ($^1H-^1H$ COSY), and Varian XL 500 (^1H, ^{13}C, and $^1H-^{13}C$ heteronuclear correlation) spectrometers, respectively. NMR data were reported as δ (ppm) downfield from external TMS or internal solvent.

(10) Alyea, E. C.; Malek, A.; Vougioukas, A. E. *Can. J. Chem.* **1982**, *60*, 667.
(11) Smith, A.; Rettig, S. J.; Orvig, C. *Inorg. Chem.* **1988**, *27*, 3929.
(12) Berg, D. J.; Rettig, S. J.; Orvig, C. *J. Am. Chem. Soc.* **1991**, *113*, 2528.
(13) Liu, S.; Gelmini, L.; Rettig, S. J.; Thompson, R. C.; Orvig, C. *J. Am. Chem. Soc.* **1992**, *114*, 6081.
(14) Sarma, B. D.; Bailar, J. C., Jr. *J. Am. Chem. Soc.* **1955**, *77*, 5476.
(15) Sarma, B. D.; Ray, K. R.; Sievers, R. E.; Bailar, J. C., Jr. *J. Am. Chem. Soc.* **1964**, *86*, 14.
(16) Isobe, T.; Kida, S.; Misumi, S. *Bull. Chem. Soc. Jpn.* **1967**, *40*, 1862.
(17) Bailey, N. A.; McKenzie, E. D.; Worthington, J. M.; McPartlin, M.; Tasker, P. A. *Inorg. Chim. Acta* **1977**, *25*, L137.
(18) Tsang, B. W.; Mathias, C. J.; Green, M. A. *J. Nucl. Med.* **1993**, *34*, 1127.
(19) Evans, D. F.; Jakubovic, D. A. *J. Chem. Soc., Dalton Trans.* **1988**, 2927.
(20) Guerriero, P.; Vigato, P. A.; Fenton, D. E.; Hellier, P. C. *Acta Chem. Scand.* **1992**, *46*, 1025.
(21) Baraniak, E.; Bruce, R. S. L.; Freeman, H. C.; Hair, N. J.; James, J. *Inorg. Chem.* **1976**, *15*, 2226.
(22) Harrison, D.; Giorgetti, A.; Bünzli, J.-C. G. *J. Chem. Soc., Dalton Trans.* **1985**, 885.
(23) Rebizant, J.; Spirlet, M. R.; Barthelemy, P. P.; Desreux, J. F. *J. Inclusion Phenom.* **1987**, *5*, 505.
(24) Kahwa, I. A.; Folkes, S.; Williams, D. J.; Ley, S. V.; O'Mahoney, C. A.; McPherson, G. L. *J. Chem. Soc., Chem. Commun.* **1989**, 1531.
(25) Blech, P.; Floriani, C.; Chiesi-Villa, A.; Guastini, C. *J. Chem. Soc., Dalton Trans.* **1990**, 3557.
(26) Ribot, F.; Toledano, P.; Sanchez, C. *Inorg. Chim. Acta* **1991**, *185*, 239.

Mass spectra were obtained with a Kratos MS 50 (electron-impact ionization, EI), a Kratos Concept II H32Q (Cs^+ liquid secondary ion mass spectrometry, LSIMS), or an AEI MS-9 (fast atom bombardment, FAB) instrument. UV/vis spectra were recorded on a Shimadzu UV-2100 spectrometer. Melting points were measured on a Mel-Temp apparatus and were uncorrected. Analyses for C, H, and N were carried out by Mr. Peter Borda in this department.

Syntheses of Ligands. 2-(2′-Hydroxyphenyl)-1,3-bis[3′-aza-4′-(2″-hydroxyphenyl)-prop-4′-en-1′-yl]-1,3-imidazolidine (H_3api). This was synthesized by a literature preparation[16] with some modification. A solution of 2.92 g (20 mmol) of trien in 20 mL of ethanol was added to a solution of 7.32 g (60 mmol) of salicylaldehyde in 10 mL of ethanol. A bright yellow precipitate formed immediately. The product was isolated by filtration, washed with diethyl ether and dried at room temperature for a yield of 6.8 g (75%), mp 101−103 °C. Anal. Calcd (found) for $C_{27}H_{30}N_4O_3$: C, 70.72 (70.40); H, 6.59 (6.49); N, 12.22 (12.02). Mass spectrum (EI): *m/z* 458 ($M^+ = H_3api^+$). Infrared spectrum (cm^{-1}, KBr disk): 1637 (vs, $\nu_{C=N}$), 1613, 1585, 1500, 1485, 1465, 1420 (vs or s, $\nu_{C=C}$). ^1H and ^{13}C NMR data are listed in the supplementary material. Recrystallization from methanol afforded X-ray quality crystals.

2-(2′-Hydroxy-5′-chlorophenyl)-1,3-bis[3′-aza-4′-(2″-hydroxy-5″-chlorophenyl)prop-4′-en-1′-yl]-1,3-imidazolidine (H_3Clapi). A solution of 2.92 g (20 mmol) of trien in 20 mL of ethanol was added to a hot solution of 9.36 g (60 mmol) of 5-chlorosalicylaldehyde in 100 mL ethanol. A yellow precipitate deposited at once. The suspension was cooled in an ice bath. The product was filtered out, washed with diethyl ether and dried at room temperature yielding 8.8 g (79%), mp 150−152.5 °C. Anal. Calcd (found) for $C_{27}H_{27}Cl_3N_4O_3$: C, 57.71 (57.40); H, 4.84 (4.88); N, 9.97 (9.73). Mass spectrum (EI): *m/z* 561 ($M^+ = H_3Clapi^+$). Infrared spectrum (cm^{-1}, KBr disk): 1647 (s, $\nu_{C=N}$), 1585, 1486, 1455 (m or s, $\nu_{C=C}$). ^1H and ^{13}C NMR data are listed in the supplementary material. Recrystallization from methanol afforded X-ray quality crystals.

2-(2′-Hydroxy-5′-bromophenyl)-1,3-bis[3′-aza-4′-(2″-hydroxy-5″-bromophenyl)-prop-4′-en-1′-yl]-1,3-imidazolidine (H_3Brapi). This was synthesized by the procedure outlined above for H_3(Clapi) using trien (2.92 g, 20 mmol) and 5-bromosalicylaldehyde (12.12 g, 60 mmol). The yield was 10.7 g (77%); mp 149−152 °C. Anal. Calcd (found) for $C_{27}H_{27}Br_3N_4O_3$: C, 46.64 (46.58); H, 3.91 (3.96); N, 8.06 (8.11). Mass spectrum (EI): *m/z* 696 ($M^+ = H_3Brapi^+$). Infrared spectrum (cm^{-1}, KBr disk): 1635 (s, $\nu_{C=N}$), 1575, 1480, 1443 (all m or s, $\nu_{C=C}$). ^1H and ^{13}C NMR data are listed in the supplementary material.

1-(2′-Hydroxybenzyl)-2,2-dimethyl-3-[3′,6′-diaza-3′-(2″-hydroxybenzyl)-7′-(2″-hydroxyphenyl)heptyl]-1,3-imidazolidine (H_3(1,2,4-ahi)). To a suspension of 6.8 g (15 mmol) of H_3api in 20 mL of methanol was added 2.7 g (50 mmol) of potassium borohydride in small portions over 30 min. The Schiff base dissolved gradually. Continued stirring for another 30 min ensured that the yellow color disappeared completely. The solution was rotary-evaporated to near dryness; to the residue was added a solution of 5.2 g of ammonium acetate in 50 mL of water. The mixture was extracted with chloroform (2 × 200 mL). The organic fractions were combined, washed with water (2 × 100 mL), dried over 16 g of anhydrous magnesium sulfate for 30 min, and clarified by filtration. Rotary evaporation of the solvents resulted in oily products, which were converted into a pale yellow solid by trituration with acetone. The yield was 1.5 g (20%); mp 86−88.5 °C. Anal. Calcd (found) for $C_{30}H_{40}N_4O_3 \cdot {}^1/_2H_2O$: C, 70.15 (70.26); H, 8.04 (7.93); N, 10.91 (10.93). Infrared spectrum (cm^{-1}, KBr disk): 3700−2100 (br s, $\nu_{N-H,\ O-H}$), 1615 (m), 1595 (s) (δ_{N-H}); 1490 (vs), 1460 (s) ($\nu_{C=C}$). ^1H NMR ($CDCl_3$): 7.24−6.65 (m, phenyl, 12H); 3.82 (s, benzyl H, 2H); 3.72 (s, benzyl H, 2H); 3.70 (s, benzyl H, 2H); 2.81(s) and 2.68(d) (NCH_2CH_2N, 12H); 1.18 (s, CH_3, 6H). The simplified resonances for the backbone hydrogens and benzylic hydrogens suggested that the compound was a mixture of acetone adducts H_3(1,2,4-btt) and byproduct H_3(1,1,4-btt) (which was subsequently proven by X-ray structures, *vide infra*). Mass spectrum (FAB): *m/z* 506 (M^+ = mixture of $[H_4(1,2,4\text{-ahi})]^+$ and $[H_4(1,1,4\text{-ahi})]^+$), 465 ($M^+$ = mixture of $[H_4(1,2,4\text{-btt})]^+$ and $[H_4(1,1,4\text{-btt})]^+$).

In order to obtain an NMR spectrum of the purified ligand H_3(1,2,4-btt), decomposition of the complex Yb(1,2,4-btt) was employed. Yb(1,2,4-btt) (0.0308 g) was dissolved in 9 mL of HCl (0.1 M) and a trisodium phosphate (0.145 g) in a small amount of water was added; a white precipitate formed immediately. This solid was removed by filtration and washed with chloroform. The aqueous solution was extracted with chloroform (3 × 15 mL), and the organic fractions were combined and dried over anhydrous magnesium sulphate for 15 min. Rotary evaporation of the solvent gave a yellow oil of pure H_3(1,2,4-btt). ^1H NMR ($CDCl_3$): 7.34−6.71 (m, phenyl, 12H); 5.42 (br s, OH, 3H); 3.96 (s, benzyl H, 2H); 3.77 (s, benzyl H, 2H); 3.68 (s, benzyl H, 2H); 2.72−2.60 (m, NCH_2CH_2N, 12H). Reaction of acetone with the pure H_3(1,2,4-btt) gave the pure H_3(1,2,4-ahi). ^1H NMR ($CDCl_3$): 7.2−6.6 (m, phenyl, 12H); 4.00−3.54 (m, benzyl H, 6H); 2.92−2.42 (m, NCH_2CH_2N, 12H); 1.22 (s, CH_3, 3H); 1.12 (s, CH_3, 3H).

Syntheses of Lanthanide and Indium Complexes. Since many of the syntheses were similar, detailed procedures were given only for representative examples. All lanthanide complexes and their IR spectral and mass (FAB or LSIMS) data are listed in Table 1. Analytical data (CHN, satisfactory for all complexes) and ^1H NMR data for $[La(Xapi)]_2$ are reported in supplementary material.

$[Ln(Xapi)]_2 \cdot mH_2O$. Method 1. A solution of H_3Xapi (0.5 mmol) in 20 mL of chloroform was added to a solution of $Ln(NO_3)_3 \cdot nH_2O$ (0.5 mmol) in 100 mL of methanol. The mixture was neutralized with 0.35 g of sodium acetate (excess). The solution was kept at room temperature for several days while tiny crystals formed; the solvent was then decanted. The product was rinsed with water, ethanol and diethyl ether, and dried at room temperature; mp > 200 °C dec. Only the lanthanum complexes were soluble in chloroform. The mass spectra of the other $[Ln(Xapi)]_2 \cdot mH_2O$ complexes could not be obtained because of their low solubilities in common solvents or matrices. The infrared spectra of the $[Ln(Xapi)]_2 \cdot mH_2O$ complexes were almost superimposible in the 1400−1700 cm^{-1} region with that of $[La(Xapi)]_2$. Crystals of $[La(Brapi)]_2$ suitable for X-ray diffraction were obtained by dissolving the pure complex in chloroform and inducing crystallization by the diffusion of methanol.

Method 2. A solution of H_3Xapi (0.5 mmol) in 20 mL of chloroform was added to a solution of $Ln(NO_3)_3 \cdot nH_2O$ (0.5 mmol) in 100 mL of methanol. The solution was kept at room temperature for about 1 week, and the solvent was then decanted. The product was rinsed with water, ethanol and diethyl ether, and dried at room temperature. Characterization showed these products to be identical to those obtained by method 1.

$[La(H_3Xapi)(NO_3)_3]$. To a solution of the respective ligand H_3-Xapi (0.5 mmol) in 10 mL of chloroform was added dropwise a solution of $La(NO_3)_3 \cdot 6H_2O$ (0.5 mmol) in 10 mL of methanol. The mixture was poured into 100 mL of diethyl ether and the yellow solid precipitated immediately. The product was washed with chloroform, and diethyl ether, and dried on a vacuum line at 60 °C for one week, mp > 200 °C dec.

$[Ln(H_3Xapi)(NO_3)_3] \cdot mH_2O$ (Ln = Gd, Yb). To a solution of Ln-$(NO_3)_3 \cdot mH_2O$ (0.5 mmol) in 10 mL of methanol was added a solution of H_3Xapi (0.5 mmol) in 10 mL of chloroform, and a yellow powder precipitated at once. The product was isolated by filtration, washed with chloroform and diethyl ether, and dried at room temperature; mp > 200 °C dec. The infrared spectra of the $Ln(H_3Xapi)(NO_3)_3$ complexes were almost superimposible in the 1400−1700 cm^{-1} region with that of $La(H_3Xapi)(NO_3)_3$. The complexes were insoluble in chloroform, and slightly soluble in methanol and ethanol; they demetalated in DMSO.

{*N*,*N*′,*N*‴-Tris(2-oxobenzyl)triethylenetetramine}ytterbium(III), Yb(1,2,4-btt). A solution of 0.25 g (0.5 mmol) of the product of the KBH_4 reduction of H_3api (a mixture of H_3(1,1,4-ahi) and H_3-(1,2,4-ahi)) in 20 mL of chloroform was mixed with a solution of 0.22 g (0.5 mmol) of $Yb(NO_3)_3 \cdot 5H_2O$ in 25 mL of methanol. The solution became cloudy on the addition of a solution of 0.06 g of NaOH and was filtered immediately. Keeping the solution at room temperature for several days yielded colorless, platelike crystals suitable for X-ray diffraction. The solvent was decanted, and the product was dried with diethyl ether; mp > 200 °C dec. The infrared spectra of the Ln(1,2,4-btt) complexes were almost superimposible in the 1400−1700 cm^{-1} region with that of Yb(1,2,4-btt). The solubilities of the complexes in common organic solvents were so low (μM) as to be observed only by UV/vis.

Table 1. Molecular Formula (from Elemental Analysis−CHN), Mass Spectral Data, and Infrared Spectral Data (cm^{-1}, KBr disk) for the Lanthanide Complexes of the Various Schiff Base and Amine Phenol Ligands

complex	*m/z*	IR bands
$[La(api)]_2$	1189 ($[H(ML)_2]^+$); 595 ($[HML]^+$)	1622 vs ($\nu_{C=N}$); 1600 s, 1540 s, 1480 vs, 1470 vs, 1450 s ($\nu_{C=C}$)
$[Pr(api)]_2$		1630 vs ($\nu_{C=N}$); 1600 s, 1540 s, 1478 vs, 1470 vs, 1455 vs ($\nu_{C=C}$)
$[Nd(api)]_2 \cdot 2H_2O$		1630 vs ($\nu_{C=N}$); 1600 vs, 1540 s, 1478 vs, 1470 vs, 1455 vs ($\nu_{C=C}$)
$[Gd(api)]_2 \cdot H_2O$		1635 vs ($\nu_{C=N}$); 1600 s, 1542 m, 1481 s, 1474 vs, 1458 s ($\nu_{C=C}$)
$[Yb(api)]_2 \cdot 2H_2O$		1630 vs ($\nu_{C=N}$); 1605 vs, 1540 s, 1474 vs, 1455 vs ($\nu_{C=C}$)
$La(H_3api)(NO_3)_3 \cdot 0.5Et_2O$	1189 ($[H(ML)_2]^+$); 721 ($[M(H_3L)(NO_3)_2]^+$); 595 ($[HML]^+$)	1648 vs ($\nu_{C=N}$); 1607 s, 1536 s, 1496−1438 br s ($\nu_{C=C}$); 1290 vs ($\nu_{NO_3^-}$)
$Gd(H_3api)(NO_3)_3 \cdot 0.5H_2O$	614 ($[HML]^+$)	1652 vs ($\nu_{C=N}$); 1610 s, 1540 s, 1485 vs ($\nu_{C=C}$); 1390 vs, 1290 vs ($\nu_{NO_3^-}$)
$Yb(H_3api)(NO_3)_3$	756 ($[M(H_3L)(NO_3)_2]^+$); 630 ($[HML]^+$)	1652 s ($\nu_{C=N}$); 1610 m, 1540 m, 1487 s ($\nu_{C=C}$); 1388 s, 1300 m ($\nu_{NO_3^-}$)
$[La(Clapi)]_2$	1395 ($[H(ML)_2]^+$); 697 ($[HML]^+$)	1630 vs ($\nu_{C=N}$); 1598 w, 1532 s, 1471 vs, 1425 w ($\nu_{C=C}$)
$[Pr(Clapi)]_2$		1630 vs ($\nu_{C=N}$); 1598 w, 1530 s, 1470 vs, 1422 w ($\nu_{C=C}$)
$[Nd(Clapi)]_2$		1630 vs ($\nu_{C=N}$); 1600 w, 1532 s, 1474 vs, 1422 w ($\nu_{C=C}$)
$[Gd(Clapi)]_2 \cdot CHCl_3$		1630 vs ($\nu_{C=N}$); 1598 w, 1530 s, 1470 vs, 1422 w ($\nu_{C=C}$)
$[Yb(Clapi)]_2 \cdot 2H_2O$		1630 vs ($\nu_{C=N}$); 1600 w, 1532 s, 1474 vs, 1422 w ($\nu_{C=C}$)
$La(H_3Clapi)(NO_3)_3 \cdot 0.5Et_2O$	1395 ($[H(ML)_2]^+$); 823 ($[M(H_3L)(NO_3)_2]^+$); 697 ($[HML]^+$)	1648 vs ($\nu_{C=N}$); 1606 w, 1521 s, 1484 vs ($\nu_{C=C}$); 1286 s ($\nu_{NO_3^-}$)
$Gd(H_3Clapi)(NO_3)_3 \cdot H_2O$	718 ($[HML]^+$)	1652 vs ($\nu_{C=N}$); 1615 w, 1528 s, 1507−1450 br vs ($\nu_{C=C}$); 1388 s, 1300 br s ($\nu_{NO_3^-}$)
$Yb(H_3Clapi)(NO_3)_3 \cdot H_2O$	734 ($[HML]^+$)	1654 vs ($\nu_{C=N}$); 1613 w, 1529 s, 1490 vs ($\nu_{C=C}$); 1390 vs, 1300 br s($\nu_{NO_3^-}$)
$[La(Brapi)]_2$	1663 ($[H(ML)_2]^+$); 831 ($[HML]^+$)	1630 vs ($\nu_{C=N}$); 1589 s, 1528 s, 1480 vs, 1470 vs, 1419 w ($\nu_{C=C}$)
$[Pr(Brapi)]_2$		1625 vs ($\nu_{C=N}$); 1589 m, 1530 m, 1470 vs, 1418 w ($\nu_{C=C}$)
$[Nd(Brapi)]_2$		1625 vs ($\nu_{C=N}$); 1590 m, 1530 m, 1470 vs, 1420 w($\nu_{C=C}$)
$[Gd(Brapi)]_2 \cdot 3H_2O$		1627 vs ($\nu_{C=N}$); 1590 m, 1530 s, 1470 vs, 1420 w ($\nu_{C=C}$)
$[Yb(Brapi)]_2 \cdot 2H_2O$		1630 vs ($\nu_{C=N}$); 1590 m, 1530 m, 1470 vs, 1420 w ($\nu_{C=C}$)
$La(H_3Brapi)(NO_3)_3 \cdot 2.5MeOH$	831 ($[HML]^+$)	1648 vs ($\nu_{C=N}$); 1605 w, 1518 s, 1476 vs ($\nu_{C=C}$); 1286 br vs ($\nu_{NO_3^-}$)
$Gd(H_3Brapi)(NO_3)_3$	850 ($[HML]^+$)	1650 vs ($\nu_{C=N}$); 1608 m, 1521 s, 1480 br vs ($\nu_{C=C}$); 1390 m, 1300 br vs ($\nu_{NO_3^-}$)
$Yb(H_3Brapi)(NO_3)_3$	992 ($[M(H_3L)(NO_3)_2]^+$); 866 ($[HML]^+$)	1650 vs ($\nu_{C=N}$); 1610 w, 1520 s, 1480 vs ($\nu_{C=C}$); 1388 vs, 1290 s ($\nu_{NO_3^-}$)
$La(H_3(1,2,4\text{-btt}))(NO_3)_3 \cdot MeOH$	1201 ($[H(ML)_2]^+$); 863 ($[M_2L(NO_3)_2]^+$); 601 ($[HML]^+$)	1590 m (δ_{N-H}); 1473 vs, 1450 vs ($\nu_{C=C}$); 1380 vs, 1300 br s ($\nu_{NO_3^-}$)
$Gd(H_3(1,2,4\text{-btt}))(NO_3)_3 \cdot 0.5Et_2O$	1238 ($[H(ML)_2]^+$); 618 ($[HML]^+$)	1593 s (δ_{N-H}); 1480 vs, 1450 vs ($\nu_{C=C}$); 1300−1260 br vs ($\nu_{NO_3^-}$)
$Yb(H_3(1,2,4\text{-btt}))(NO_3)_3 \cdot 0.5Et_2O$	931 ($[M_2L(NO_3)_2]^+$); 636 ($[HML]^+$)	1595 s (δ_{N-H}); 1480 vs, 1450 vs ($\nu_{C=C}$); 1380 m, 1300 vs ($\nu_{NO_3^-}$)
$La(1,2,4\text{-btt}).CHCl_3 \cdot 2H_2O$	601 ($[HML]^+$)	1595 s, 1563 m (δ_{N-H}); 1482 vs, 1451 vs ($\nu_{C=C}$)
$Gd(1,2,4\text{-btt}) \cdot 0.5H_2O$	618 ($[HML]^+$)	1595 s, 1562 w (δ_{N-H}); 1480 vs, 1450 s ($\nu_{C=C}$)
$Yb(1,2,4\text{-btt})$	635 ($[HML]^+$)	1598 vs, 1565 m (δ_{N-H}); 1488 vs, 1455 vs ($\nu_{C=C}$)

$[Ln(H_3(1,2,4\text{-btt}))(NO_3)_3]$. To a solution of $Ln(NO_3)_3 \cdot nH_2O$ (0.5 mmol) in 10 mL of methanol was added a solution of $H_3(1,2,4\text{-ahi})$ (0.5 mmol) in 10 mL of methylene chloride. Upon addition of diethyl ether, a white powder precipitated at once. This product was isolated by filtration, washed with methylene chloride and diethyl ether, and dried on a vacuum line at 60 °C for 1 week; mp > 200 °C dec. The infrared spectra of the $Ln(H_3(1,2,4\text{-btt}))(NO_3)_3$ complexes were almost superimposible with $La(H_3(1,2,4\text{-btt}))(NO_3)_3$ in the 1400−1700 cm^{-1} region. The complexes were insoluble in chloroform, methylene chloride, and somewhat soluble in methanol.

{*N,N,N‴*-Tris(2-oxobenzyl)triethylenetetramine}indium(III), In-(1,1,4-btt). To a solution of $In(NO_3)_3 \cdot 5H_2O$ (0.395 g, 1.0 mmol) in methanol (5 mL) was added a solution of the product from KBH_4 reduction of H_3api (0.5 g, 1.1 mmol) in methanol (20 mL). Aqueous 2N NaOH solution (2 mL) was then added. The solution was then filtered immediately and the filtrate allowed to evaporate slowly at room temperature. Slow evaporation of the solvent produced crystals suitable for X-ray diffraction studies. These were separated by filtration, washed with ethanol and diethyl ether, and dried in air. The yield was 350 mg (61%). Anal. Calcd (found) for $C_{27}H_{33}InN_4O_3 \cdot 0.5H_2O$: C, 55.40 (55.32); H, 5.85 (5.82); N, 9.57 (9.57). Mass spectrum (FAB): *m/z* 1153 ($M^+ = [H(In(1,1,4\text{-btt}))_2]^+$); 577 ($M^+ = [HIn(1,1,4\text{-btt})]^+$). IR($cm^{-1}$ KBr disk): 3500−3360 (br, w, ν_{OH}); 3260 (w, ν_{NH}); 1595 and 1565 (s and m, δ_{NH}).

Autoconversion of Capped Schiff Base Complexes to Sandwich Dimer Schiff Base Complexes. All the sandwich dimer complexes can be obtained through a spontaneous conversion from a capped tridentate ligand structure, only representative spectra are given in Figures 2 and 3. $Gd(H_3api)(NO_3)_3$ was dissolved in methanol (0.3 mM), and the solution was monitored over 7 days at room temperature in the range 240−600 nm.

X-ray Crystallographic Analyses of H_3api, H_3Clapi, Yb(1,2,4-btt)·0.5MeOH, In(1,1,4-btt), and $[La(Brapi)]_2 \cdot 2CHCl_3$. Selected crystallographic data for the five structures appear in Table 2. The final unit cell parameters were obtained by least-squares on the setting angles for 25 reflections with $2\theta = 39.0-85.3°$ for H_3api, 45.1−59.8° for H_3Clapi, 30.5−53.0° for $[La(Brapi)]_2 \cdot 2CHCl_3$, 28.3−33.5° for Yb-(1,2,4-btt)·0.5MeOH, and 63.4−78.2° for In(1,1,4-btt). The intensities of three standard reflections (measured every 200 reflections throughout the data collections) remained constant for H_3api, H_3Clapi, and Yb-(1,2,4-btt)·0.5MeOH, and decayed linearly for $[La(Brapi)]_2 \cdot 2CHCl_3$ (4.3%) and In(1,1,4-btt) (2.7%). The data were processed[27] and corrected for Lorentz and polarization effects, decay (for $[La(Brapi)]_2 \cdot 2CHCl_3$ and In(1,1,4-btt)), and absorption (empirical, based on azimuthal scans for three reflections).

The structures of H_3api, H_3Clapi, and $[La(Brapi)]_2 \cdot 2CHCl_3$ were solved by direct methods and those of the Yb and In complexes by the Patterson method. The structure analyses of H_3Clapi, $[La(Brapi)]_2 \cdot 2CHCl_3$, and In(1,1,4-btt) were initiated in the centrosymmetric space groups *Pnma*, *C2/c*, and $P\bar{1}$, rather than the respective noncentrosymmetric space groups $Pn2_1a$, *Cc*, and *P*1 that exhibit the same systematic absences, on the basis of the *E*-statistics. These choices were confirmed by subsequent calculations. The H_3Clapi is situated on a crystallographic mirror plane, but the central aromatic ring is (1:1) disordered with respect to the mirror plane by a rotation about the C(2)−C(3) bond. This arrangement allows for the formation of an intramolecular O(1)−H(1)···N(1) hydrogen bond like that observed in the ordered H_3api molecule. The disordered atoms Cl(1), O(1), C(4), C(5), and C(8) were resolved, but C(7) could not be successfully refined when moved off the mirror plane. Refinement in the lower symmetry noncentrosymmetric space group $Pn2_1a$ failed to resolve the disorder problem. The $[La(Brapi)]_2$ complex is situated about a center of symmetry at ($^1/_4$, $^1/_4$, 0) and the asymmetric unit contains one molecule of chloroform. The asymmetric unit of the Yb complex contains two Yb(1,2,4-btt) molecules and a methanol molecule. The oxygen atom of the methanol solvate is (74:26) 2-fold disordered. The site occupancy factors for the two components of the disordered oxygen atom were originally estimated from relative Fourier map peak heights and were adjusted as the refinement progressed to give approximately equal equivalent isotropic thermal parameters. Attempts to refine the

(27) *teXsan: Crystal Structure Analysis Package*; Molecular Structure Corporation: The Woodlands, TX, 1985 & 1992.

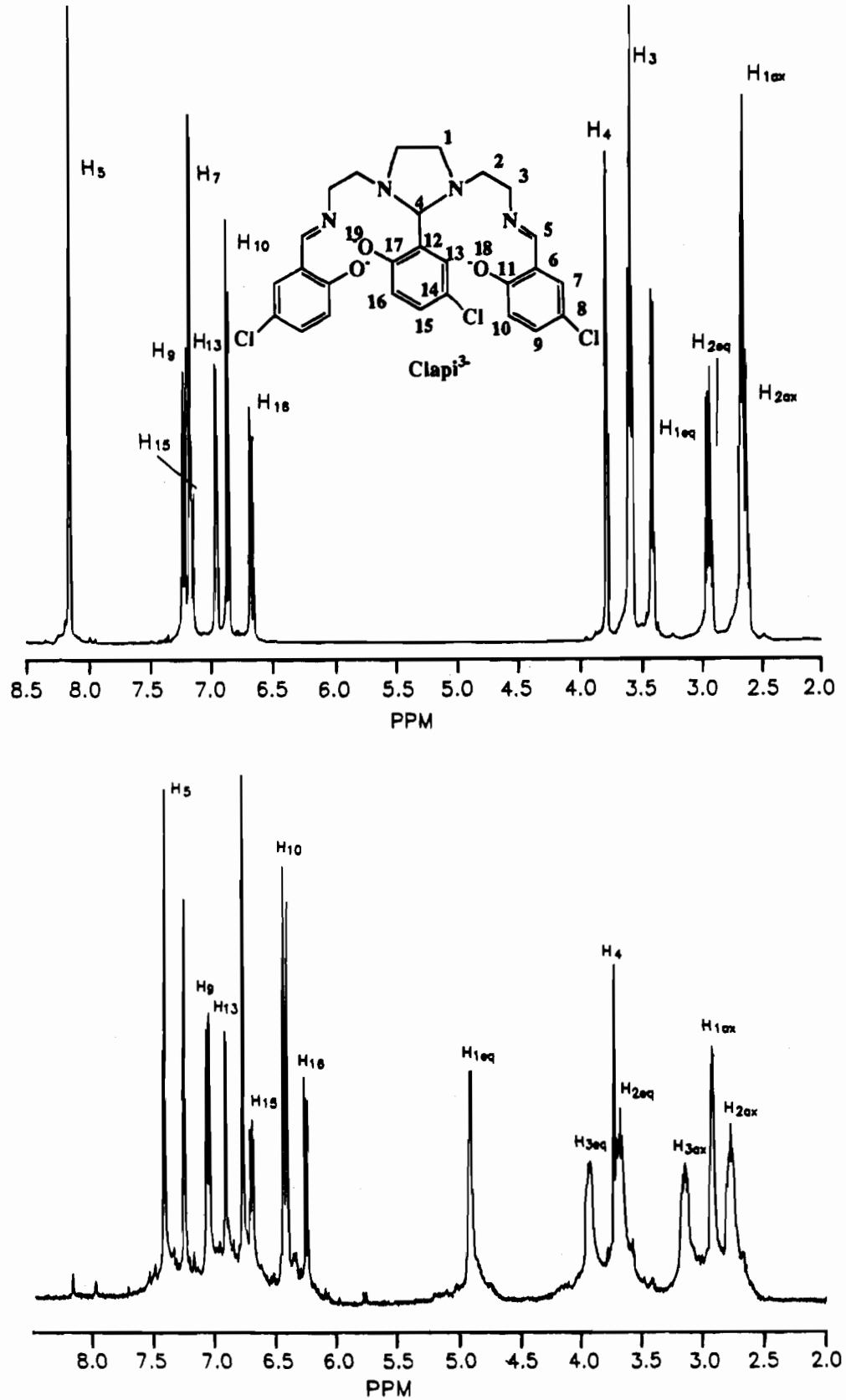

Figure 1. ^1H NMR spectra (400 MHz) of H_3Clapi (top) and $[La(Clapi)]_2$ (bottom) in $CDCl_3$ at room temperature.

occupancy factors resulted in physically unreasonable thermal parameters. The asymmetric unit of In(1,1,4-btt) contains two independent molecules.

All non-hydrogen atoms except for the low-occupancy methanol oxygen atom, O(4a), of H_3Clapi were refined with anisotropic thermal parameters. The OH hydrogen atoms in H_3api and H_3Clapi were refined with isotropic thermal parameters. The remaining hydrogen atoms in each of the structures were fixed in calculated positions (N−H/C−H = 0.98 Å, $B_H = 1.2B_{\text{bonded atom}}$). Secondary extinction corrections were applied for H_3api, H_3Clapi, and In(1,1,4-btt), the final values of the extinction coefficients being $2.17(5) \times 10^{-6}$, $8.3(2) \times 10^{-7}$, and $8.9(2) \times 10^{-7}$, respectively. Neutral atom scattering factors for all atoms[28] and anomalous dispersion corrections for the non-hydrogen atoms[29] were taken from the *International Tables for X-Ray Crystallography*.

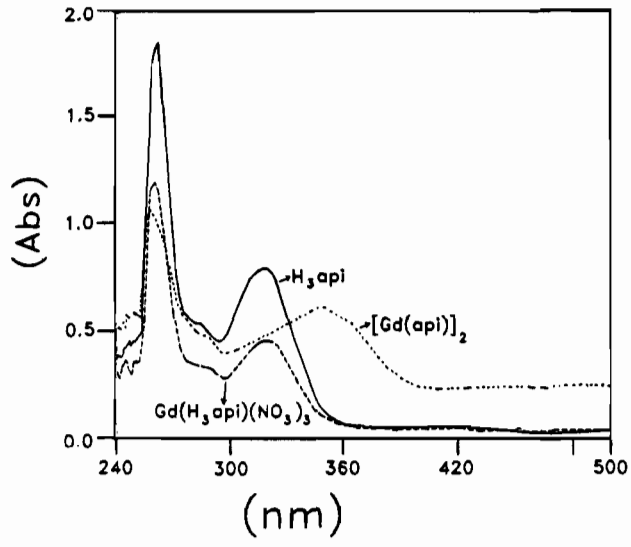

Figure 2. UV/vis spectra of H_3api, Gd(H_3api)(NO_3)$_3$, and [Gd(api)]$_2$ in DMSO at room temperature. Gd(H_3api)(NO_3)$_3$ slowly decomposes in DMSO, while [Gd(api)]$_2$ is stable.

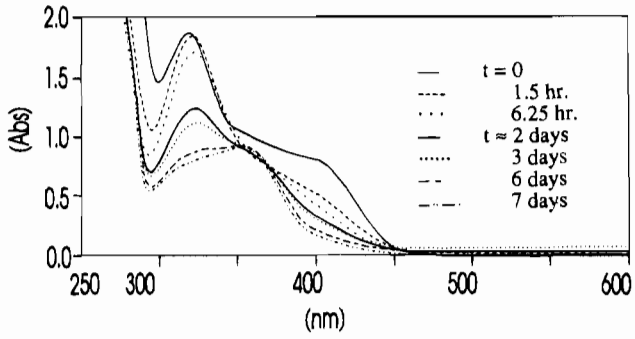

Figure 3. UV/vis spectra of the spontaneous conversion of 0.3 mM Gd(H_3api)(NO_3)$_3$ to [Gd(api)]$_2$ at room temperature in methanol.

Selected bond lengths and bond angles for each of the five structures appear in Tables 3–7, and appropriate ORTEP diagrams are found in Figures 4–8. Complete tables of crystallographic data, final atomic coordinates and equivalent isotropic thermal parameters, bond lengths, bond angles, anisotropic thermal parameters, hydrogen atom parameters, intermolecular contacts, and least-squares planes for the structures, as well as a listing of measured and calculated structure factor amplitudes, are included as supplementary material (see paragraph at end of paper).

Results and Discussion

Three potentially heptadentate Schiff bases were prepared by the condensation of trien with 3 equiv of salicylaldehyde or 5-substituted salicylaldehyde (Scheme 1). A mixture of the isomeric amine phenols H_3(1,2,4-btt) and H_3(1,1,4-btt) was obtained by the KBH_4 reduction of H_3api. Pure H_3(1,2,4-btt) was obtained by the decompositon of its Yb complex.

^{1}H and ^{13}C NMR spectral assignments for the Schiff bases were based on ^{1}H–^{1}H COSY and ^{1}H–^{13}C heteronuclear correlation with the attached proton test (APT), and were consistent with the proposed formulations (the ^{1}H NMR spectrum of H_3Clapi is shown as part of Figure 1). Infrared spectra of the Schiff bases showed peaks around 1640 cm^{-1}, which are characteristic of imine C=N bonds. It is noted that in these Schiff bases, five-membered imidazolidine rings were formed at the backbone after the condensation and that the middle arm was therefore unique from the other two arms (clearly shown in the ^{1}H NMR spectra). Two phenolic OH resonances were observed at about 10 and 13 ppm in a 1:2 ratio. These two downfield signals can be explained by the intramolecular hydrogen bonding of the phenolic OH with an unsaturated azomethine nitrogen or tertiary nitrogen which causes a decrease in the shielding at the hydroxy hydrogen. However the OH resonances on the terminal outside arms are further downfield than that of the middle arm. The explanation is that, for the terminal arm, the O–H---N group lies coplanar with the aromatic ring (proven in the X-ray structures, *vide infra*); hence, the proton is further deshielded by the induced aromatic ring current, as has been seen before in related studies.[30]

Borohydride reduction of the unsubstituted Schiff base H_3-api suggested that the final pure H_3(1,2,4-ahi) was the acetone adduct of H_3(1,2,4-btt) (the oily product, proven by ^{1}H NMR). This suggestion was supported by the FAB mass spectrum which showed two peaks, at *m/z* 506 (for [H_4(1,2,4-ahi)]$^+$) and *m/z* 465 (for [H_4(1,2,4-btt)]$^+$). The infrared spectra showed the disappearance of the C=N band at 1637 cm^{-1} and the appearance of two new bands at 1595 and 1615 cm^{-1}, due to N–H bending vibrations. The ^{1}H NMR data indicated the absence of CH=N hydrogen resonances at about 8 ppm and the presence of new benzylic CH_2 resonances at about 4 ppm, confirming the reduction of the unsubstituted Schiff bases. Comparison of the ^{1}H NMR data between H_3(1,2,4-btt) and its acetone adduct H_3(1,2,4-ahi) showed a large difference for the benzylic hydrogen resonances. In H_3(1,2,4-btt), three identical peaks for the benzylic hydrogens appeared because of the asymmetric nature of the molecule. After the formation of the adduct, the three peaks became a complex series of multiplets engendered by the rigidity of the five-membered imidazolidine ring preventing the free rotation of the benzylic carbon of one end and differentiating the two hydrogens on that carbon. This rigidity also resulted in the inequivalency of the two methyl groups (originating from acetone), which gave two singlets in the ^{1}H NMR spectrum. Reduction of the two 5-substituted (Cl, Br) Schiff bases to make H_3ahi analogs showed that the microanalyses were consistent with the reduced formulations, but the complex ^{1}H NMR spectra suggested that these products were mixtures of isomers; efforts to purify these compounds were unsuccessful.

The five-membered imidazolidine ring formed in the Schiff base condensation opened during the reduction, which likely resulted in the middle arm migration (Scheme 2). The identified by-product was the ligand H_3(1,1,4-btt) as shown in the X-ray structure of In(1,1,4-btt). This can be explained by the formation of stabilized iminium ions present in protic solvents[31] (Scheme 2). The C=N linkages on the terminal arms are reduced first, then the lone pairs on the secondary nitrogens begin to attack the carbon to form intermediate *b*. The intermediate *(b)* can either give the product H_3(1,2,4-btt) through reduction, or form another intermediate *(c)*, which leads to the minor by-product H_3(1,1,4-btt). After acetone addition, another five-membered imidazolidine ring was formed at the backbone. As will be discussed later, the five-membered ring formed in the reduction will reopen, and H_3(1,2,4-ahi) will appear as (1,2,4-btt)$^{3-}$ after complexing.

Study of reactions of lanthanides with potentially heptadentate N_4O_3 ligands has revealed four coordination types (Chart 1):

(28) *International Tables for Crystallography*; The Kynoch Press: Birmingham, UK (present distributor: Kluwer Academic Publisher: Boston, MA), 1974; Vol. IV, p 99.
(29) *International Tables for Crystallography*; Kluwer Academic Publishers: Boston, MA, 1992; Vol. C, p 219.
(30) Gündüz, N.; Gündüz, T.; Hursthouse, M. B.; Parkes, H. G.; Shaw, L. S.; Shaw, R. A.; Tüzün, M. *J. Chem. Soc., Perkin Trans. 2* **1985**, 899.
(31) Salerno, A.; Ceriani, V.; Perillo, I. A. *J. Heterocycl. Chem.* **1992**, *29*, 1725.

Table 2. Selected Crystallographic Data[a]

	H_3api	H_3Clapi	[La(Brapi)]$_2$·2CHCl$_3$	Yb(1,2,4-btt)·0.5MeOH	In(1,1,4-btt)
formula	$C_{27}H_{30}N_4O_3$	$C_{27}H_{27}Cl_3N_4O_3$	$C_{56}H_{50}Br_6Cl_6La_2N_8O_6$	$C_{27.5}H_{35}N_4O_{3.5}Yb$	$C_{27}H_{33}InN_4O_3$
fw	458.56	561.89	1901.01	650.64	576.40
cryst syst	monoclinic	orthorhombic	monoclinic	monoclinic	triclinic
space group	$P2_1/a$	$Pnma$	$C2/c$	$P2_1/n$	$P\bar{1}$
a, Å	19.281(2)	11.398(4)	22.336(1)	12.798(2)	12.771(2)
b, Å	5.774(3)	21.486(3)	14.770(2)	19.671(6)	18.994(4)
c, Å	21.999(2)	10.942(4)	22.647(2)	21.129(2)	11.450(2)
α, deg	90	90	90	90	105.71(1)
β, deg	97.85(1)	90	116.855(5)	91.895(9)	99.73(1)
γ, deg	90	90	90	90	89.21(2)
V, Å^3	2426(1)	2680(2)	6665.7(9)	5316(1)	2633.7(8)
Z	4	4	4	8	4
ϱ_{calc}, g/cm^3	1.255	1.393	1.894	1.626	1.454
T, °C	21	21	21	21	21
radiation	Cu	Cu	Cu	Mo	Cu
λ, Å	1.541 78	1.541 78	1.541 78	0.710 69	1.541 78
μ, cm^{-1}	6.32	34.51	166.28	35.43	75.93
transm factors (rel)	0.96−1.00	0.85−1.00	0.59−1.00	0.46−1.00	0.53−1.00
R	0.034	0.035	0.042	0.031	0.029
R_w	0.031	0.032	0.036	0.025	0.035

[a] $R = \sum||F_o| - |F_c||/\sum|F_o|$, $R_w = (\sum w(|F_o| - |F_c|)^2/\sum w|F_o|^2)^{1/2}$.

Table 3. Selected Bond Lengths (Å) and Angles (deg) in H_3api with Estimated Standard Deviations

Bond Lengths			
O(1)−C(9)	1.364(3)	N(4)−C(7)	1.457(3)
O(2)−C(16)	1.358(3)	N(4)−C(21)	1.277(2)
O(3)−C(23)	1.359(3)	C(1)−C(8)	1.507(3)
N(1)−C(1)	1.471(2)	C(2)−C(3)	1.496(3)
N(1)−C(2)	1.457(3)	C(4)−C(5)	1.517(3)
N(1)−C(4)	1.459(3)	C(6)−C(7)	1.507(3)
N(2)−C(1)	1.489(2)	C(8)−C(9)	1.393(3)
N(2)−C(3)	1.480(3)	C(14)−C(15)	1.448(3)
N(2)−C(6)	1.461(3)	C(15)−C(16)	1.392(3)
N(3)−C(5)	1.464(3)	C(21)−C(22)	1.455(3)
N(3)−C(14)	1.271(3)	C(22)−C(23)	1.390(3)

Bond Angles			
C(1)−N(1)−C(2)	104.4(2)	C(1)−C(8)−C(13)	119.8(2)
C(1)−N(1)−C(4)	112.3(2)	C(9)−C(8)−C(13)	118.2(2)
C(2)−N(1)−C(4)	113.1(2)	O(1)−C(9)−C(8)	121.3(2)
C(1)−N(2)−C(3)	106.8(2)	O(1)−C(9)−C(10)	118.4(2)
C(1)−N(2)−C(6)	113.3(2)	C(8)−C(9)−C(10)	120.2(2)
C(3)−N(2)−C(6)	112.7(2)	N(3)−C(14)−C(15)	122.2(2)
C(5)−N(3)−C(14)	118.3(2)	C(14)−C(15)−C(16)	121.6(2)
C(7)−N(4)−C(21)	119.2(2)	C(14)−C(15)−C(20)	120.0(2)
N(1)−C(1)−N(2)	103.4(2)	C(16)−C(15)−C(20)	118.3(2)
N(1)−C(1)−C(8)	111.2(2)	O(2)−C(16)−C(15)	121.3(2)
N(2)−C(1)−C(8)	113.9(2)	O(2)−C(16)−C(17)	118.8(3)
N(1)−C(2)−C(3)	102.7(2)	C(15)−C(16)−C(17)	119.9(2)
N(2)−C(3)−C(2)	105.5(2)	N(4)−C(21)−C(22)	121.4(2)
N(1)−C(4)−C(5)	110.7(2)	C(21)−C(22)−C(23)	121.1(2)
N(3)−C(5)−C(4)	109.8(2)	C(21)−C(22)−C(27)	120.3(3)
N(2)−C(6)−C(7)	112.7(2)	C(23)−C(22)−C(27)	118.7(2)
N(4)−C(7)−C(6)	108.1(2)	O(3)−C(23)−C(22)	121.5(2)
C(1)−C(8)−C(9)	121.9(2)	O(3)−C(23)−C(24)	118.1(3)
		C(22)−C(23)−C(24)	120.4(2)

Table 4. Selected Bond Lengths (Å) and Angles (deg) in H_3Clapi with Estimated Standard Deviations

Bond Lengths			
O(1)−C(4)	1.353(6)	C(1)−C(1)[a]	1.504(6)
O(2)−C(13)	1.346(3)	C(2)−C(3)	1.507(5)
N(1)−C(1)	1.482(3)	C(3)−C(4)	1.418(5)
N(1)−C(2)	1.462(3)	C(9)−C(10)	1.511(4)
N(1)−C(9)	1.455(3)	C(11)−C(12)	1.453(4)
N(2)−C(10)	1.456(4)	C(12)−C(13)	1.404(4)
N(2)−C(11)	1.269(3)		

Bond Angles			
C(1)−N(1)−C(2)	103.4(2)	O(1)−C(4)−C(5)	118.4(5)
C(1)−N(1)−C(9)	113.7(2)	C(3)−C(4)−C(5)	119.2(5)
C(2)−N(1)−C(9)	113.7(2)	N(1)−C(9)−C(10)	112.8(2)
C(10)−N(2)−C(11)	118.5(3)	N(2)−C(10)−C(9)	111.4(2)
N(1)−C(1)−C(1)[a]	104.6(1)	N(2)−C(11)−C(12)	122.8(3)
N(1)−C(2)−N(1)[a]	100.8(3)	C(11)−C(12)−C(13)	120.9(3)
N(1)−C(2)−C(3)	113.9(2)	C(11)−C(12)−C(17)	120.3(3)
C(2)−C(3)−C(4)	120.6(4)	C(13)−C(12)−C(17)	118.7(3)
C(2)−C(3)−C(8)	120.3(4)	O(2)−C(13)−C(12)	121.4(3)
C(4)−C(3)−C(8)	118.8(4)	O(2)−C(13)−C(14)	119.1(3)
O(1)−C(4)−C(3)	122.3(4)	C(12)−C(13)−C(14)	119.6(3)

[a] Symmetry operation: x, $^1/_2 - y$, z.

encapsulated,[12] capped tridentate,[11] encapsulated dimer,[13] and bicapped.[32] We have again found the first two types, as well as a new sandwich dimer structure. Homodinuclear lanthanide complexes with the formulation [Ln(Xapi)]$_2$ were prepared from reactions of Ln^{3+} with these potentially heptadentate Schiff bases in the presence of excess weak base (acetate). These sandwich complexes could also be prepared from the reaction of a lanthanide nitrate salt with 1 equiv of the Schiff base because of the instability of the capped Schiff base complexes and their autoconversion to sandwich dimer complexes. The new sandwich dimer complexes have been characterized by IR spectroscopy and elemental analysis (^{1}H NMR, mass spectrometry and UV/vis spectroscopy are only available for the lanthanum complexes), and, for [La(Brapi)]$_2$·2CHCl$_3$, by X-ray crystallography.

These homodinuclear complexes contain two lanthanide ions; instead of forcing N_4O_3 donor atoms from one ligand onto one metal ion as reported for the encapsulated dimers,[13] each of the metal ions is coordinated by two N_2O donor sets, one from one ligand, one from another. Two phenolate O atoms, from the middle arm of each ligand, act as bridges between the two metal centers and complete the coordination sphere, and the sandwich dimer structure. Compared to the infrared spectra of capped complexes, the O−H and NO_3^- bands disappeared in the sandwich dimers, and the C=N frequencies underwent bathochromic shifts upon coordination to the metal ions. A comparison of the ^{1}H NMR spectra between the ligand H_3Clapi and its complex [La(Clapi)]$_2$ in $CDCl_3$ is shown in Figure 1. In H_3Clapi, the 5-membered ring enforces considerable rigidity, which results in two different hydrogen resonances for both H_1's and H_2's; the end arm can freely rotate, and only one signal is observed for the two H_3's. After coordinating the metal ions, both the backbone and the arms are more rigid (i.e. much more restricted rotationally), the singlet of the two H_3 hydrogens is

(32) Liu, S.; Yang, L.-W.; Rettig, S. J.; Orvig, C. *Inorg. Chem.* **1993**, *32*, 2773.

Table 5. Selected Bond Lengths (Å) and Angles (deg) in One of the Two Independent Molecules of Yb(1,2,4-btt) with Estimated Standard Deviations

Bond Lengths			
Yb(1)−O(1)	2.160(3)	N(3)−C(4)	1.481(6)
Yb(1)−O(2)	2.145(3)	N(3)−C(5)	1.477(6)
Yb(1)−O(3)	2.170(3)	N(4)−C(6)	1.474(6)
Yb(1)−N(1)	2.485(4)	N(4)−C(21)	1.482(7)
Yb(1)−N(2)	2.551(4)	C(1)−C(2)	1.524(7)
Yb(1)−N(3)	2.470(4)	C(3)−C(4)	1.506(6)
Yb(1)−N(4)	2.483(4)	C(5)−C(6)	1.497(8)
O(1)−C(9)	1.322(5)	C(7)−C(8)	1.507(7)
O(2)−C(16)	1.339(6)	C(8)−C(9)	1.409(6)
O(3)−C(23)	1.338(6)	C(14)−C(15)	1.510(7)
N(1)−C(1)	1.474(6)	C(15)−C(16)	1.397(7)
N(1)−C(7)	1.502(6)	C(21)−C(22)	1.508(7)
N(2)−C(2)	1.485(6)	C(22)−C(23)	1.399(7)
N(2)−C(3)	1.495(6)	O(4)−C(28)	1.36(1)
N(2)−C(14)	1.511(5)		

Bond Angles			
O(1)−Yb(1)−O(2)	169.4(1)	Yb(1)−N(3)−C(4)	108.0(3)
O(1)−Yb(1)−O(3)	98.7(1)	Yb(1)−N(3)−C(5)	110.9(3)
O(1)−Yb(1)−N(1)	80.4(1)	C(4)−N(3)−C(5)	113.7(4)
O(1)−Yb(1)−N(2)	98.9(1)	Yb(1)−N(4)−C(6)	112.1(3)
O(1)−Yb(1)−N(3)	82.7(1)	Yb(1)−N(4)−C(21)	113.6(3)
O(1)−Yb(1)−N(4)	77.7(1)	C(6)−N(4)−C(21)	113.6(4)
O(2)−Yb(1)−O(3)	88.1(1)	N(1)−C(1)−C(2)	111.1(4)
O(2)−Yb(1)−N(1)	108.8(1)	N(2)−C(2)−C(1)	112.4(4)
O(2)−Yb(1)−N(2)	80.0(1)	N(2)−C(3)−C(4)	111.8(4)
O(2)−Yb(1)−N(3)	87.2(1)	N(3)−C(4)−C(3)	107.3(4)
O(2)−Yb(1)−N(4)	96.0(1)	N(3)−C(5)−C(6)	107.9(5)
O(3)−Yb(1)−N(1)	81.2(1)	N(4)−C(6)−C(5)	108.9(4)
O(3)−Yb(1)−N(2)	143.1(1)	N(1)−C(7)−C(8)	113.4(4)
O(3)−Yb(1)−N(3)	146.3(1)	C(7)−C(8)−C(9)	120.0(5)
O(3)−Yb(1)−N(4)	77.8(1)	C(7)−C(8)−C(13)	120.6(5)
N(1)−Yb(1)−N(2)	70.2(1)	C(9)−C(8)−C(13)	119.4(5)
N(1)−Yb(1)−N(3)	131.7(1)	O(1)−C(9)−C(8)	120.4(5)
N(1)−Yb(1)−N(4)	146.7(1)	O(1)−C(9)−C(10)	121.5(5)
N(2)−Yb(1)−N(3)	68.2(1)	C(8)−C(9)−C(10)	118.1(5)
N(2)−Yb(1)−N(4)	137.8(1)	N(2)−C(14)−C(15)	114.8(4)
N(3)−Yb(1)−N(4)	69.6(1)	C(14)−C(15)−C(16)	120.6(5)
Yb(1)−O(1)−C(9)	134.0(3)	C(14)−C(15)−C(20)	120.4(5)
Yb(1)−O(2)−C(16)	134.4(3)	C(16)−C(15)−C(20)	118.8(5)
Yb(1)−O(3)−C(23)	132.5(3)	O(2)−C(16)−C(15)	120.6(5)
Yb(1)−N(1)−C(1)	115.6(3)	O(2)−C(16)−C(17)	120.0(5)
Yb(1)−N(1)−C(7)	109.5(3)	C(15)−C(16)−C(17)	119.4(5)
C(1)−N(1)−C(7)	112.9(4)	N(4)−C(21)−C(22)	110.7(4)
Yb(1)−N(2)−C(2)	106.4(3)	C(21)−C(22)−C(23)	120.1(5)
Yb(1)−N(2)−C(3)	112.6(3)	C(21)−C(22)−C(27)	120.6(6)
Yb(1)−N(2)−C(14)	109.3(3)	C(23)−C(22)−C(27)	119.2(6)
C(2)−N(2)−C(3)	108.8(4)	O(3)−C(23)−C(22)	121.3(5)
C(2)−N(2)−C(14)	109.5(4)	O(3)−C(23)−C(24)	120.6(5)
C(3)−N(2)−C(14)	110.1(4)	C(22)−C(23)−C(24)	118.2(5)

split into two multiplets assigned to H_{3eq} and H_{3ax}, and the peak for H_5 of CH=N moves upfield while the peaks for H_{1eq} and H_{2eq} move downfield as far as 4.9 and 3.68 ppm, from 3.40 and 2.93 ppm in the ligand, respectively. (Assignments of H_{ax} and H_{eq} are tentative and are distinguished by the fact that the hydrogens in pseudoaxial environments are usually more shielded than those in pseudoequatorial environments.[33]) Unlike those for other unstable Schiff base lanthanide complexes, the UV/vis spectra of the sandwich dimer lanthanide complexes in DMSO showed that the complexes are quite hydrolytically stable in this strongly coordinating solvent (Figure 2). This unusual property can also be explained by the restricted rotation of the ligands. Martell and Hancock[34] have noted that addition of C-methyl groups to the ethylene bridge of EDTA decreases the rotation of the ligand and gives complexes of

Table 6. Selected Bond Lengths (Å) and Angles (deg) in One of the Two Independent Molecules of In(1,1,4-btt) with Estimated Standard Deviations

Bond Lengths			
In(1)−O(1)	2.163(2)	N(2)−C(17)	1.468(5)
In(1)−O(2)	2.104(2)	N(3)−C(18)	1.468(5)
In(1)−O(3)	2.111(2)	N(3)−C(19)	1.458(5)
In(1)−N(1)	2.368(3)	N(4)−C(20)	1.472(5)
In(1)−N(2)	2.428(3)	N(4)−C(21)	1.488(5)
In(1)−N(3)	2.472(3)	C(1)−C(2)	1.502(5)
In(1)−N(4)	2.340(3)	C(2)−C(3)	1.409(5)
O(1)−C(3)	1.310(4)	C(8)−C(9)	1.510(5)
O(2)−C(10)	1.332(4)	C(9)−C(10)	1.404(5)
O(3)−C(23)	1.332(4)	C(15)−C(16)	1.514(5)
N(1)−C(1)	1.505(5)	C(17)−C(18)	1.509(6)
N(1)−C(8)	1.481(4)	C(19)−C(20)	1.511(5)
N(1)−C(15)	1.497(4)	C(21)−C(22)	1.501(5)
N(2)−C(16)	1.466(5)	C(22)−C(23)	1.414(5)

Bond Angles			
O(1)−In(1)−O(2)	90.3(1)	In(1)−N(3)−C(18)	113.2(2)
O(1)−In(1)−O(3)	98.5(1)	In(1)−N(3)−C(19)	113.5(2)
O(1)−In(1)−N(1)	78.64(9)	C(18)−N(3)−C(19)	114.4(3)
O(1)−In(1)−N(2)	151.3(1)	In(1)−N(4)−C(20)	116.0(2)
O(1)−In(1)−N(3)	138.63(9)	In(1)−N(4)−C(21)	108.6(2)
O(1)−In(1)−N(4)	72.3(1)	C(20)−N(4)−C(21)	114.8(3)
O(2)−In(1)−O(3)	169.87(9)	N(1)−C(1)−C(2)	115.9(3)
O(2)−In(1)−N(1)	87.1(1)	C(1)−C(2)−C(3)	122.0(3)
O(2)−In(1)−N(2)	89.9(1)	C(1)−C(2)−C(7)	118.5(4)
O(2)−In(1)−N(3)	79.3(1)	C(3)−C(2)−C(7)	119.4(4)
O(2)−In(1)−N(4)	100.0(1)	O(1)−C(3)−C(2)	123.2(3)
O(3)−In(1)−N(1)	89.6(1)	O(1)−C(3)−C(4)	119.1(4)
O(3)−In(1)−N(2)	80.0(1)	C(2)−C(3)−C(4)	117.6(4)
O(3)−In(1)−N(3)	97.2(1)	N(1)−C(8)−C(9)	115.7(3)
O(3)−In(1)−N(4)	87.6(1)	C(8)−C(9)−C(10)	121.4(3)
N(1)−In(1)−N(2)	72.7(1)	C(8)−C(9)−C(14)	119.6(4)
N(1)−In(1)−N(3)	139.5(1)	C(10)−C(9)−C(14)	119.0(4)
N(1)−In(1)−N(4)	150.0(1)	O(2)−C(10)−C(9)	123.2(3)
N(2)−In(1)−N(3)	69.3(1)	O(2)−C(10)−C(11)	118.8(3)
N(2)−In(1)−N(4)	135.8(1)	C(9)−C(10)−C(11)	118.0(3)
N(3)−In(1)−N(4)	70.4(1)	N(1)−C(15)−C(16)	112.9(3)
In(1)−O(1)−C(3)	135.8(2)	N(2)−C(16)−C(15)	108.6(3)
In(1)−O(2)−C(10)	126.5(2)	N(2)−C(17)−C(18)	108.3(3)
In(1)−O(3)−C(23)	122.7(2)	N(3)−C(18)−C(17)	109.1(3)
In(1)−N(1)−C(1)	108.0(2)	N(3)−C(19)−C(20)	108.4(3)
In(1)−N(1)−C(8)	109.6(2)	N(4)−C(20)−C(19)	111.9(3)
In(1)−N(1)−C(15)	112.1(2)	N(4)−C(21)−C(22)	113.7(3)
C(1)−N(1)−C(8)	109.9(3)	C(21)−C(22)−C(23)	120.1(3)
C(1)−N(1)−C(15)	105.9(3)	C(21)−C(22)−C(27)	121.0(3)
C(8)−N(1)−C(15)	111.1(3)	C(23)−C(22)−C(27)	118.8(3)
In(1)−N(2)−C(16)	112.3(2)	O(3)−C(23)−C(22)	122.1(3)
In(1)−N(2)−C(17)	114.0(2)	O(3)−C(23)−C(24)	119.9(3)
C(16)−N(2)−C(17)	113.2(3)	C(22)−C(23)−C(24)	117.9(3)

uniformly higher complex stability. We expect that these dimer complexes have high stabilities, also.

There are three geometries available to the eight-coordinated metal ion: cube, square antiprism, and dodecahedron. These forms are energetically very similar and the cube can be easily distorted to an antiprism or dodecahedron by interligand repulsions;[35] generally steric nonrigidity is observed. In order to examine the fluxionalities of the sandwich dimer complexes, variable temperature ^{1}H NMR spectra of $[La(Clapi)]_2$ in DMSO-d_6 were obtained between 20 and 100 °C. There were no significant changes in the spectral parameters except for some very minor shifts in the signals; these shifts are probably caused by thermal vibrations of the coordinated ligand framework. This observation showed that the structure remained the same, undergoing no fluxional processes and confirming its rigidity, greater than that of the LnDOTA complex.[36]

(33) Silverstein, R. M.; Bassler, G. C.; Morrill, T. C. *Spectrometric Identification of Organic Compounds*, 4th ed.; John Wiley & Sons: New York, 1981.
(34) Hancock, R. D.; Martell, A. E. *Chem. Rev.* **1989**, *89*, 1875.
(35) Greenwood, N. N.; Earnshaw, A. *Chemistry of the Elements*; Pergamon Press: Oxford, England, 1984.
(36) Desreux, J. F. *Inorg. Chem.* **1980**, *19*, 1319.

Table 7. Selected Bond Lengths (Å) and Angles (deg) in $[La(Brpi)]_2$ with Estimated Standard Deviation

Bond Lengths			
La(1)−La(1)[a]	4.023(1)	La(1)−O(1)	2.451(6)
La(1)−O(1)[a]	2.466(5)	La(1)−O(2)	2.342(7)
La(1)−O(3)[a]	2.324(7)	La(1)−N(1)	2.879(8)
La(1)−N(2)[a]	2.902(7)	La(1)−N(3)	2.617(8)
La(1)−N(4)[a]	2.607(9)	O(1)−C(9)	1.334(10)
O(2)−C(16)	1.30(1)	O(3)−C(23)	1.30(1)
N(1)−C(1)	1.49(1)	N(1)−C(3)	1.47(1)
N(1)−C(4)	1.48(1)	N(2)−C(1)	1.48(1)
N(2)−C(2)	1.49(1)	N(2)−C(6)	1.48(1)
N(3)−C(5)	1.45(1)	N(3)−C(14)	1.28(1)
N(4)−C(7)	1.47(1)	N(4)−C(21)	1.29(1)
C(1)−C(8)	1.50(1)	C(2)−C(3)	1.53(1)
C(4)−C(5)	1.50(1)	C(6)−C(7)	1.52(1)
C(8)−C(9)	1.38(1)	C(21)−C(22)	1.46(1)
C(14)−C(15)	1.45(1)	C(15)−C(16)	1.40(1)
C(22)−C(23)	1.42(1)		
Bond Angles			
O(1)−La(1)−O(1)[a]	70.2(2)	O(1)−La(1)−O(2)	83.7(2)
O(1)−La(1)−O(3)[a]	144.8(2)	O(1)−La(1)−N(1)	69.0(2)
O(1)−La(1)−N(2)[a]	82.9(2)	O(1)−La(1)−N(3)	109.7(2)
O(1)−La(1)−N(4)[a]	142.6(3)	O(1)[a]−La(1)−O(2)	143.0(2)
O(1)[a]−La(1)−O(3)[a]	84.8(2)	O(1)[a]−La(1)−N(1)	83.9(2)
O(1)[a]−La(1)−N(2)[a]	68.7(2)	O(1)[a]−La(1)−N(3)	143.8(3)
O(1)[a]−La(1)−N(4)[a]	110.6(2)	O(2)−La(1)−O(3)[a]	128.8(2)
O(2)−La(1)−N(1)	111.3(2)	O(2)−La(1)−N(2)[a]	82.8(2)
O(2)−La(1)−N(3)	69.2(2)	O(2)−La(1)−N(4)[a]	75.0(3)
O(3)[a]−La(1)−N(1)	84.5(2)	O(3)[a]−La(1)−N(2)[a]	111.2(2)
O(3)[a]−La(1)−N(3)	76.4(3)	O(3)[a]−La(1)−N(4)[a]	68.9(3)
N(1)−La(1)−N(2)[a]	146.2(2)	N(1)−La(1)−N(3)	64.0(3)
N(1)−La(1)−N(4)[a]	147.6(3)	N(2)[a]−La(1)−N(3)	147.1(2)
N(2)[a]−La(1)−N(4)[a]	64.4(3)	N(3)−La(1)−N(4)[a]	91.2(3)
La(1)−O(1)−La(1)[a]	109.8(2)	La(1)−O(1)−C(9)	122.8(6)
La(1)[a]−O(1)−C(9)	118.9(5)	La(1)−O(2)−C(16)	135.1(8)
La(1)[a]−O(3)−C(23)	137.3(7)	La(1)−N(1)−C(1)	118.5(5)
La(1)−N(1)−C(3)	105.7(6)	La(1)−N(1)−C(4)	108.6(6)
C(1)−N(1)−C(3)	105.0(8)	C(1)−N(1)−C(4)	107.7(8)
C(3)−N(1)−C(4)	111.2(8)	La(1)[a]−N(2)−C(1)	118.3(5)
La(1)[a]−N(2)−C(2)	105.9(6)	La(1)[a]−N(2)−C(6)	107.1(6)
C(1)−N(2)−C(2)	104.8(8)	C(1)−N(2)−C(6)	108.0(7)
C(2)−N(2)−C(6)	112.9(8)	La(1)−N(3)−C(5)	113.0(6)
La(1)−N(3)−C(14)	128.7(8)	C(5)−N(3)−C(14)	118.3(10)
La(1)[a]−N(4)−C(7)	111.8(8)	La(1)[a]−N(4)−C(21)	129.6(8)
C(7)−N(4)−C(21)	118(1)	N(1)−C(1)−N(2)	103.9(7)
N(1)−C(1)−C(8)	113.7(8)	N(2)−C(1)−C(8)	114.2(8)
N(2)−C(2)−C(3)	106.4(8)	N(1)−C(3)−C(2)	105.6(8)
N(1)−C(4)−C(5)	113.4(9)	N(3)−C(5)−C(4)	108.5(9)
N(2)−C(6)−C(7)	113.2(9)	N(4)−C(7)−C(6)	107(1)
C(1)−C(8)−C(9)	122.3(8)	C(1)−C(8)−C(13)	117(1)
C(9)−C(8)−C(13)	120(1)	O(1)−C(9)−C(8)	121.4(10)
O(1)−C(9)−C(10)	120(1)	C(8)−C(9)−C(10)	118.3(9)
N(3)−C(14)−C(15)	126.9(10)	C(14)−C(15)−C(16)	122.6(10)
C(14)−C(15)−C(20)	115(1)	C(16)−C(15)−C(20)	121(1)
O(2)−C(16)−C(15)	124(1)	O(2)−C(16)−C(17)	118(1)
C(15)−C(16)−C(17)	116.9(9)	N(4)−C(21)−C(22)	124(1)
C(21)−C(22)−C(23)	122(1)	C(21)−C(22)−C(27)	115(1)
C(23)−C(22)−C(27)	121(1)	O(3)−C(23)−C(22)	123(1)
O(3)−C(23)−C(24)	121(1)	C(22)−C(23)−C(24)	114(1)

[a] Symmetry operation: $^1/_2 - x, ^1/_2 - y, -z$.

Reaction of a Schiff base with 1 equiv of a lanthanide salt in a small volume of solvent in the absence of a weak base produces mononuclear complexes with the formulation $[Ln(H_3Xapi)(NO_3)_3]$ in which the ligand is tridentate and capped (Chart 1). The sequence of the addition of the starting materials is very important for the lanthanum complexes. When a solution of ligand was added to a solution of the lanthanum ion, impure product mixtures always resulted despite extensive washing with chloroform to remove possible impurities—the ligand and, possibly, the sandwich $[LnL]_2$ complex. When the sequence was reversed, the analyses of the La complexes fit the formulation. UV/vis spectra of these complexes in methanol were different from those of ligands, suggesting the coordination of the ligands to the metal ions. In DMSO the UV/vis spectra showed the spectrum of the free ligand. In this strong σ-donor solvent, the complexes seem to decompose to form solvated Ln^{3+} species. The infrared spectra of these complexes showed two bidentate nitrate bands around 1390 and 1300 cm^{-1}. Broad bands at 3700−2200 cm^{-1} belong to O−H stretching vibrations in the protonated ligands. C=N groups were not coordinated and their IR bands moved upfield compared to those in the ligands (because of delocalization, coordination of phenol oxygen resulted in a stronger azomethine bond). New bands below 600 cm^{-1} were likely to be ν_{Ln-O} or ν_{Ln-N}; however, assignments of these bands are very difficult in this region because of the low energies associated with these vibrations.[37] These observations are similar to those of the previously reported nine coordinate capping ligand complexes.[11]

The mass spectra (3-nitrobenzyl alcohol matrix, positive-ion detection mode) of the sandwich dimers of La and the capped $[Ln(H_3L)(NO_3)_3]$ of all the lanthanides were obtained (Table 1). In the spectra of the latter, base peaks corresponding to the $[HLnL]^+$ were detected and there were no molecular ion peaks. For the former, both monomeric ($[HLaXapi]^+$) and dimeric ($[H(LaXapi)_2]^+$) molecular ion peaks were detected with similar intensities. This is consistent with the structural finding for $[LaBrapi]_2 \cdot 2CHCl_3$. In the spectra of all three sadwich lanthanum dimers, there were also fragmentation patterns indicative of the respective ligand.

Unlike other stable capped complexes, the $Ln(H_3Xapi)(NO_3)_3$ complexes are air-stable but very unstable in solution and spontaneously convert to sandwich dimers. The discovery of this novel autoconversion in methanol was fortuitous. After the lanthanide salts and the ligands were mixed in a 1:1 ratio in large amount of methanol, the precipitation of the expected capped ligand complexes led unexpectedly to the recovery of the dimers. This behavior was common across the lanthanide series, and the autoconversion spectra were only recorded in detail for the Gd−H_3api system (0.3 mM) as shown in Figure 3. The first spectrum was recorded right after dissolving $Gd(H_3api)(NO_3)_3$ in methanol solution, and the subsequent spectra were recorded over seven days. The peak at 319 nm disappeared gradually and a new peak around 360 nm appeared as a precipitate of $[Gd(api)]_2$ formed. Insolubility of the product prevented further study but both the spectra in solution and the characterization of the solid product proved the autoconversion.

Reactions of an amine phenol with 1 equiv of a lanthanide nitrate in the presence of diethyl ether produced the mononuclear capped tridentate ligand complexes with the formulation $[Ln(H_3(1,2,4\text{-btt}))(NO_3)_3]$ or, in the presence of excess strong base (hydroxide), the encapsulated [Ln(1,2,4-btt)]. Mass spectral and infrared data were consistent with the appropriate formulations. Both these complexes showed IR bands at 1598−1560 cm^{-1} arising from N−H bending vibrations and molecular ions $[HLn(1,2,4\text{-btt})]^+$ were found in the mass spectra, confirming their thermal robustness. There were also fragmentation patterns indicative of the respective ligand. In(1,1,4-btt) was prepared from the isomeric mixture of amine phenol ligands in order to prove the isomeric nature of the H_3(1,1,4-btt)/H_3(1,2,4-btt) ligands and to compare coordination structural features with the Ln(1,2,4-btt) complexes. We were unable to prepare Ln(1,1,4-btt) complexes.

Selected bond lengths and bond angles for H_3api are listed in Table 3 while the ORTEP drawing is illustrated in Figure 4 and the packing pattern in Figure 5. The molecule is rendered

(37) Alyea, E. C.; Malek, A.; Vougioukas, A. E. *Can. J. Chem.* **1982**, *60*, 667.

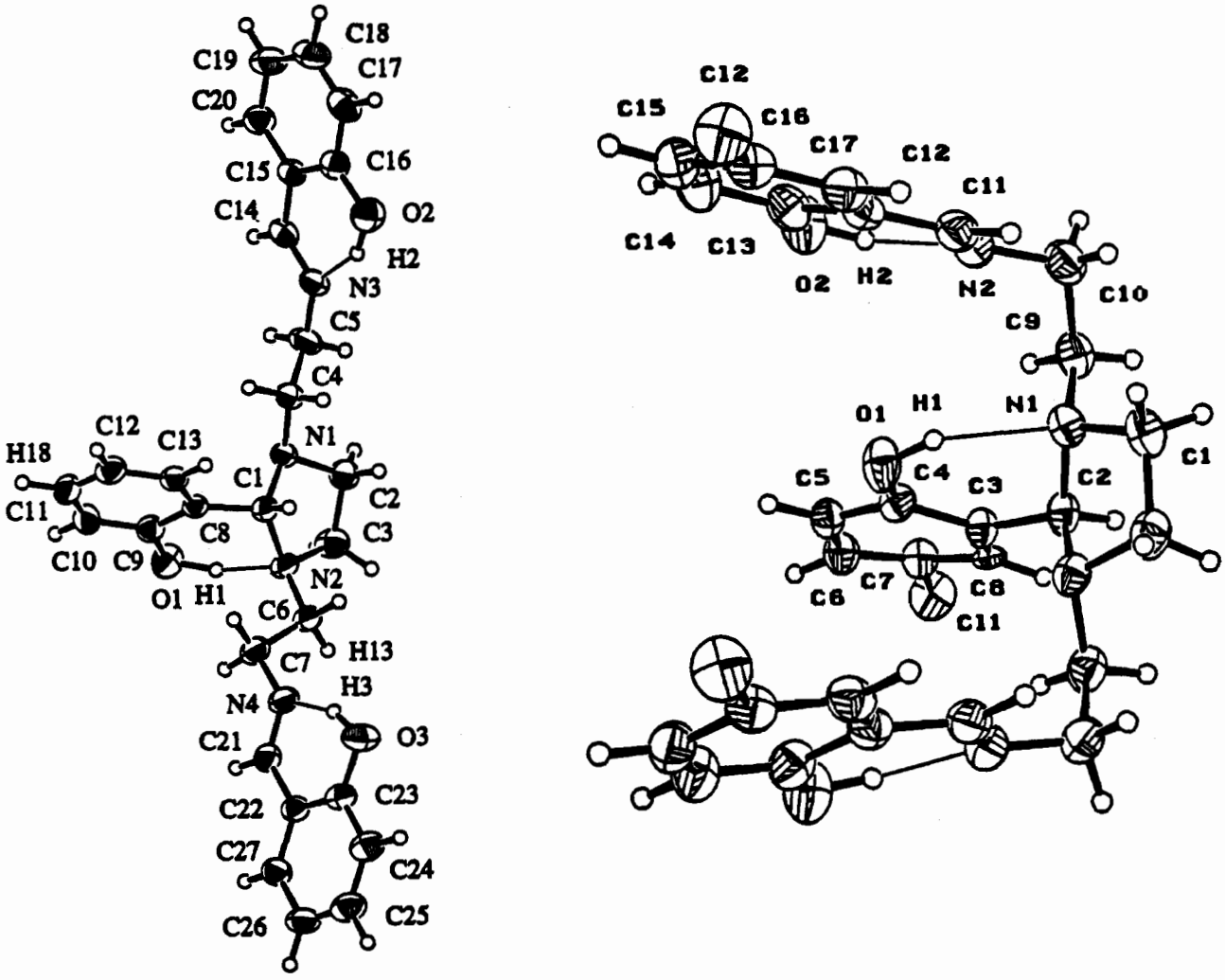

Figure 4. ORTEP drawings of H_3api (left) and H_3Clapi (right) with numbering schemes. Thermal ellipsoids for the non-hydrogen atoms are drawn at the 33% probablity level.

quite rigid by the formation of a five-membered imidazolidine ring and by the presence of three strong intramolecular hydrogen bonds (O(1)−H(1)---N(2) = O(2)−H(2)---N(3) = O(3)−H(3)---N(4) = 1.64 Å) and a very weak intermolecular hydrogen bonding interaction (C(6)−H(13)---O(3) = 2.51 Å, angle C(6)−H(13)−O(3) = 137°). The five membered imidazolidine ring adopts an envelope conformation with C(2) lying out of the plane defined by N(1), N(2), C(1), and C(3). Both N(2)−C(6)−C(7)−N(4) and N(1)−C(4)−C(5)−N(3) adopt *gauche* conformations (torsion angles: N(1)−C(4)−C(5)−N(3) = −176.6(2)°; N(2)−C(6)−C(7)−N(4) = −178.0(2)°). The whole ligand structure resembles a big T.

The intermolecular hydrogen bond distance between ethylene hydrogen (H(13)) on one molecule and oxygen (O(3)) on the terminal arm of another molecule is 2.51 Å, suggesting a C−H---O intermolecular hydrogen bonding interaction, which results in a highly ordered packing pattern (Figure 5, top). The ability of carbon atoms to act as proton donors in hydrogen bonds has been the subject of controversy for many years; however, a landmark study by Taylor and Kennard[38] in 1982 provided conclusive evidence of the existence of C−H---Y hydrogen bonds in crystals. These authors showed that C−H---Y contacts are electrostatic, the distance between the hydrogen and the acceptor atom is shorter than the sum of their van der Waals radii, and the C−H---Y angle is in the range of 90°−180°. These C−H---Y bonds are mainly found in amino acids and nucleosides.[39] The more acidic the hydrogen on the carbon atom, the more easily the C−H---Y bond can form. The H and O van der Waals radii are 1.2 and 1.5 Å, respectively. Since the H---O distance in the structure of H_3api is 2.51 Å, shorter than 2.7 Å, an intermolecular C−H---O hydrogen bonding interaction is indicated. Although there are reports on the hydrogen bonding between aromatic π hydrogen and electronegative atoms,[40] in this molecule, the intermolecular distance between O(3) and H(18) is 2.89 Å, too long to be considered a H-bond interaction. The C−H---O hydrogen bonding interaction is the main determinant in the ordered packing arrangement of this small molecule, and prevents the disorder seen in the H_3Clapi structure by enforcing the jig-saw fit of the molecules in the unit cell (compare the two packing diagrams in Figure 5).

Selected bond lengths and bond angles for H_3Clapi are listed in Table 4, and the ORTEP drawing is illustrated in Figure 4 with the packing pattern in Figure 5. Observed bond lengths for H_3Clapi are consistent with those of H_3api. As in the structure of H_3api, strong intramolecular hydrogen bonds are observed between the phenoxy hydrogens and the amine nitrogens of the trien backbone; however, there is a 50:50 disorder in the middle arm of H_3Clapi which is not observed in the structure of H_3api. The phenoxy hydrogen of this middle phenolate arm is hydrogen bonded to both the symmetry-related

(38) Taylor, R.; Kennard, O. *J. Am. Chem. Soc.* **1982**, *104*, 5063.

(39) Jeffrey, G. A.; Saenger, W. *Hydrogen Bonding in Biological Structures*; Springer-Verlag: Berlin, 1991.

(40) Atwood, J. A.; Hamada, F.; Robinson, K. D.; Orr, G. W.; Vincent, R. L. *Nature* **1991**, *349*, 683.

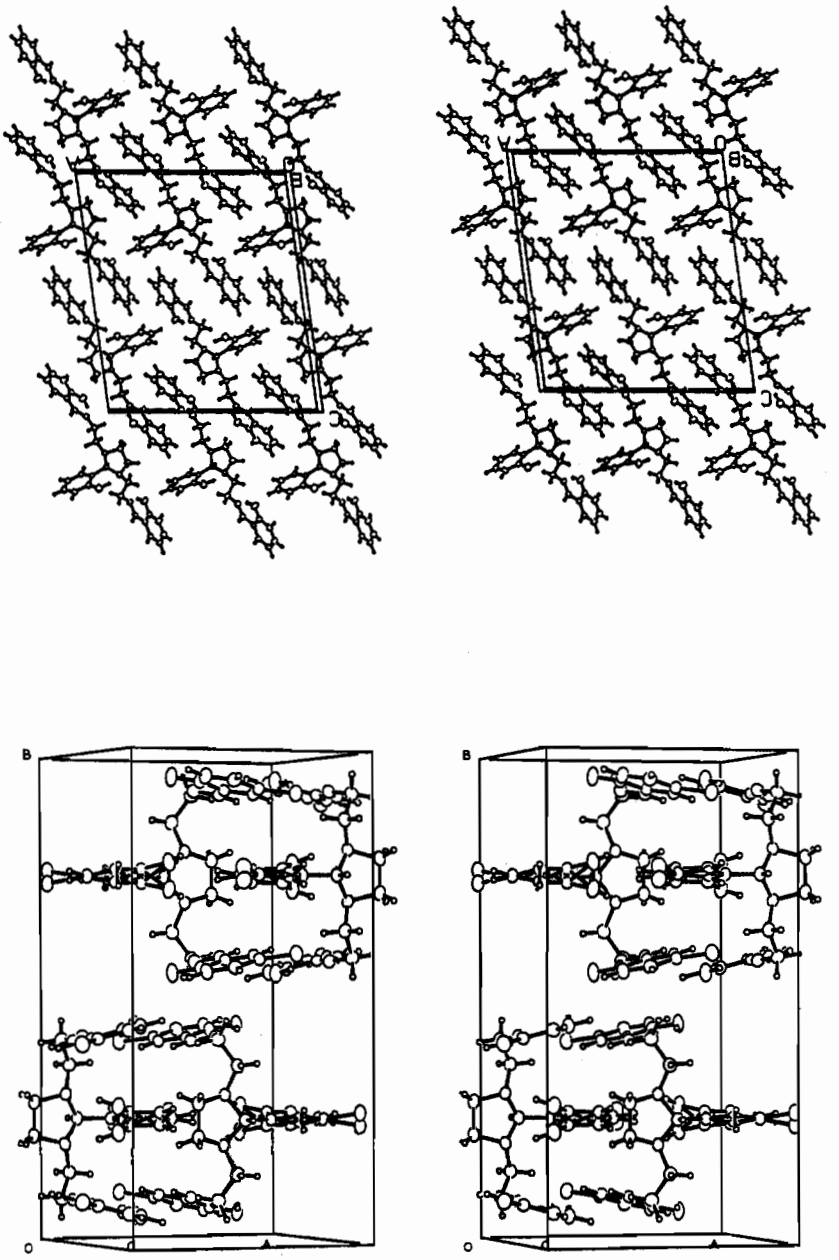

Figure 5. Stereo packing diagrams for unit cells of H_3api (top) and H_3Clapi (bottom).

imidazolidine nitrogens (N(1) and N(1)*). The hydrogen bond lengths (O(1)−H(1)---N(1) and O(1)−H(1)---N(1)*) are 2.02 Å, longer than the corresponding hydrogen bond length observed in H_3api. The hydrogen bond length O(2)−H(2)---N(2) is 1.76 Å, which is slightly longer than the corresponding hydrogen bond length in H_3api (1.64 Å). These differences in the intramolecular hydrogen bonding between the structures of H_3-api and H_3Clapi, either may cause or may result in the packing patterns of the two structures being significantly different from one another (Figure 5) since the molecules of H_3Clapi do not pack nearly as efficiently as those of H_3api into the unit cell.

The ORTEP drawing of $[La(Brapi)]_2$ is illustrated in Figure 8. Selected bond lengths and angles are listed in Table 7. The unit cell contains dinuclear $[La(Brapi)]_2$ units with two $CHCl_3$ molecules in the crystal lattice for each dimer. The complex has two identical eight-coordinated lanthanum atoms, each of which is surrounded by an N_4O_4 donor set. The two lanthanum centers are bridged by two phenolate oxygen atoms (one from each of the two middle arms of the two heptadentate ligands). The two lanthanum and two bridging oxygen atoms form a planar four-membered ring with a metal−metal separation of 4.023(1) Å and angles at the oxygen bridgehead of 109.8(2)°. The molecule is centrosymmetric. The geometry around each lanthanum atom can be viewed as a square antiprism, in which one square is composed of donor atoms O(1), O(2), N(1), and N(3), and the other of O(1)*, O(3)*, N(2)*, and N(4)*. The La−N bond lengths are 2.879(8), 2.902(7), 2.617(8), and 2.607(9) Å for La(1)−N(1), La(1)−N(2)*, La(1)−N(3), and La(1)−N(4)*, respectively, with an average of 2.751 Å. These are consistent with those found in the eight coordinated La(III) complexes of *N*-(2-(dimethylamino)ethyl)salicylideneamine[25] and 1,4,7,10-tetrakis(2-carbamoylethyl)-1,4,7,10-tetraazacyclo-dodecane.[41] The La−O bond lengths fall into two categories. The bridging La(1)−O(1)* and La(1)−O(1) distances in the four membered ring are 2.466(5) Å and 2.451(6) Å, respectively, while the terminal La−O bond lengths are 2.342(7) Å (La(1)−O(2)) and 2.324(7) Å (La(1)−O(3)*), shorter than those of Eu-O bond distances in the crystal structure of Na-(EuDOTA·H_2O)·4H_2O[42] after correction for the ionic radius

(41) Morrow, J. A.; Amin, S.; Lake, C. H.; Churchill, M. R. *Inorg. Chem.* **1993**, *32*, 4566.

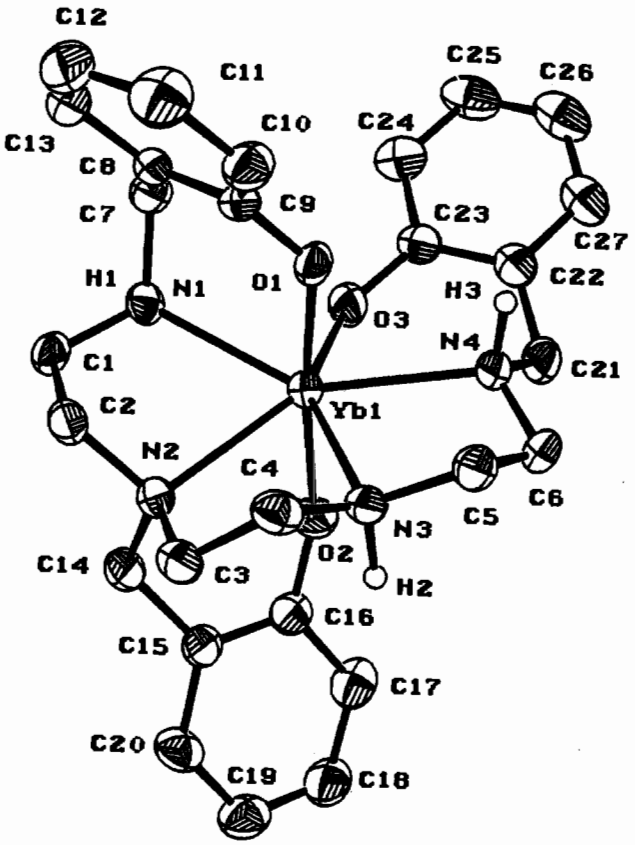

Figure 6. ORTEP drawing of one of the two independent Yb(1,2,4-btt) molecules in Yb(1,2,4-btt)·0.5MeOH. Thermal ellipsoids for the non-hydrogen atoms are drawn at the 33% probablity level.

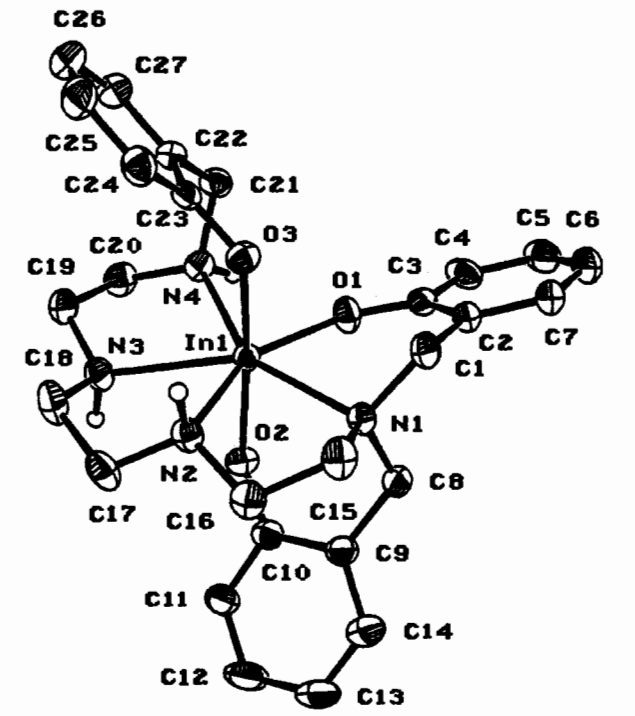

Figure 7. ORTEP drawing of one of the two independent molecules in In(1,1,4-btt). Thermal ellipsoids for the non-hydrogen atoms are drawn at the 33% probablity level.

differences of the two metal ions. Since the bridging oxygen atoms O(1) and O(1)* form two strong La−O bonds, their basicity should be lowered relative to that of the single bonded O atoms; the average bridging La−O distances (2.459 Å) are 0.126 Å longer than those of terminal La−O bonds (2.333 Å).

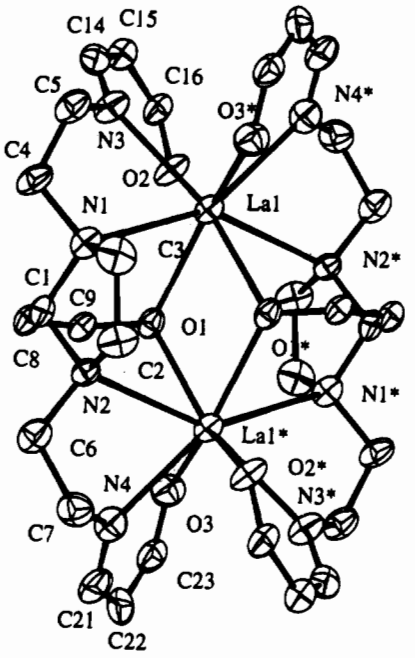

Figure 8. ORTEP drawing of $[La(Brapi)]_2$ in $[La(Brapi)]_2 \cdot 2CHCl_3$. Thermal ellipsoids for the non-hydrogen atoms are drawn at the 33% probablity level and ring atoms have been omitted for clarity.

Although the formation of a dinuclear structure is not a surprise, this new open sandwich-like structure is unexpected. This no doubt arises from the rigid five-membered imidazolidine ring in the ligand backbone; this forces the ligand into a more open configuration rendering impossible the coordination of all the donor atoms of one ligand to one metal ion. Instead, these two ligands cooperate with each other to form two compartments to accommodate two metal ions.

A single crystal structure determination of Yb(1,2,4-btt) showed this to be an encapsulated ligand complex with pentagonal bipyramidal coordination. Selected bond lengths and bond angles are listed in Table 5 and the ORTEP drawing is illustrated in Figure 6. Two independent molecules (with very slight differences in bond lengths and angles) comprise the asymmetric unit. The ligand is triply deprotonated, and all seven donor atoms (N_4O_3) are coordinated to the metal ion. The Yb−O distances average to 2.158 Å, similar to that of the Yb-(trac) complex.[12] The Yb−N distances average 2.497 Å. The bond angle between O(1)−Yb−O(2) is 169.4(1)°, consistent with these two oxygens in axial positions. After complexation, the imidazolidine ring in the ligand opened, which made the backbone and the three arms more flexible. Four nitrogens and one oxygen of a terminal arm easily wrapped around the metal ion, while the remaining two arms stretched out to occupy the axial positions. There are only a few examples[43,44] of lanthanide complexes with pentagonal bipyramidal arrangments, none of them (until now) being binary complexes with one heptadentate ligand coordinating one metal ion.

A structure determination of In(1,1,4-btt) revealed the ligand in this complex to be different from that in the Yb complex because of the migration of the middle arm to a terminal N atom (the ligands in the two complexes are structural isomers). Selected bond lengths and bond angles are listed in Table 6 and the ORTEP drawing is illustrated in Figure 7. There are

(42) Spirlet, M.-R.; Rebizant, J.; Desreux, J. F.; Loncin, M.-F. *Inorg. Chem.* **1984**, *23*, 359.
(43) Rogers, R. D.; Voss, E. J.; Etzenhouser, R. D. *Inorg. Chem.* **1988**, *27*, 533.
(44) Atwood, D. A.; Bott, S. G.; Atwood, J. L. *J. Coord. Chem.* **1987**, *17*, 93.

Scheme 2

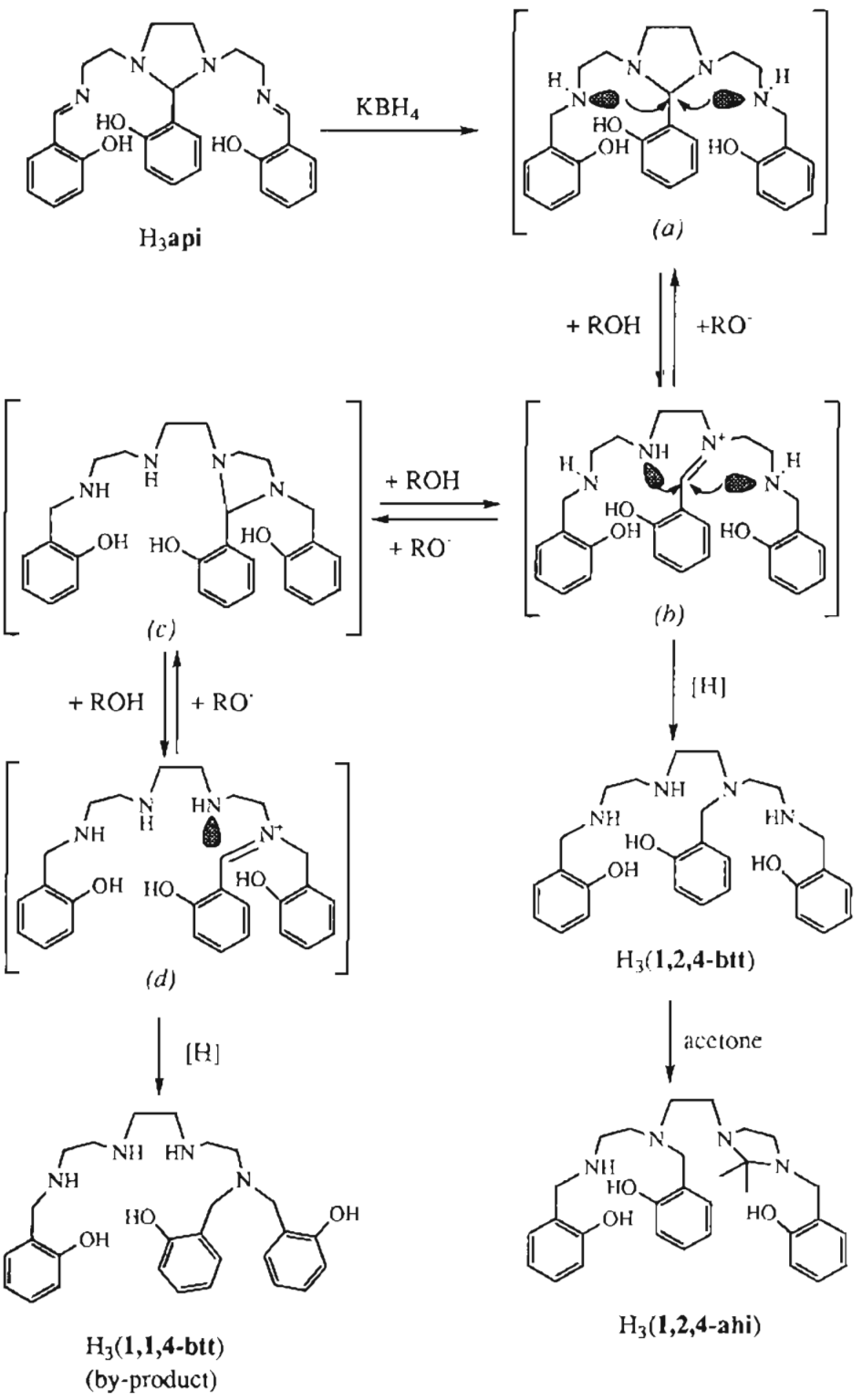

four In(1,1,4-btt) molecules (two pairs of enantiomers Λ and Δ) in the triclinic unit cell; the asymmetric unit consists of two independent molecules. In both of the independent molecules, the In ion is seven-coordinated by the triply deprotonated ligand and the geometry around the metal ion is a distorted pentagonal bipyramid. O(1), N(1), N(2), N(3), N(4), and In^{3+} are all in one plane, with two phenolate O atoms (O(2) and O(3)) axial, and the cavity fits the In^{3+} perfectly. Aside from small differences in bond lengths and bond angles in two pairs of molecules, the main difference is that in one molecule, the *trans* phenolate oxygens O(2) and O(3) are, respectively, above and below the N_3O equatorial plane whereas in the other independent molecule they are reversed, below and above. The latter orientation is shown in Figure 7.

There appear to be no undue constraints on the framework. Since Yb^{3+} (ionic radius: 0.87 Å) is a little larger than In^{3+} (ionic radius: 0.80 Å),[45] it is expected that in the Yb complex, N(1), N(2), N(3), N(4), O(3), and Yb are not all in the same plane; atoms N(3) and N(4) are above the plane, while N(2) and O(3) are below the plane. The In−O distances range from

(45) Shannon, R. D. *Acta Crystallogr.* **1976**, *A32*, 751.

2.104(2) to 2.163(2) Å, with the axial In−O bonds being slightly shorter than the equatorial In−O bond (2.10 Å vs 2.16 Å). This small difference is probably due to the reduced steric crowding in the axial position. The In−N distances range from 2.340(3) to 2.472(3) Å. The trans-axial bond angle (O(3)−In−O(2)) is 169.87(9) Å. Unlike a related seven-coordinated complex[46] of tris(2′-((hydroxybenzyl)amino)ethyl)amine, in which the tertiary nitrogen is weakly coordinated to the metal ion, all the nitrogen atoms in In(1,1,4-btt) complex form strong bonds with the ion.

Concluding Remarks. A series of Schiff bases have been prepared from the condensation reactions of various salicylaldehydes with trien, however the reduction gives different products because of the migration of a hydroxybenzyl arm. Purification of the amine phenol can be achieved by the decomposition of the resultant complex. Characterization of the Schiff base H_3api shows it to be quite rigid due to the five-membered imidazolidine ring, and inter- and intramolecular hydrogen bonding, especially the C−H---O intermolecular hydrogen bonding interactions, results in the ordered packing pattern. Unlike other Schiff base complexes, reactions of lanthanides with these rigid ligands yield new sandwich dimer complexes which are quite stable, as evinced by the novel spontaneous conversion of a capped ligand complex to a sandwich dimer complex, and by the variable temperature ^{1}H NMR of [La(Clapi)]$_2$ in DMSO-d_6 solution. Although no water is bonded to the metal ion in the sandwich dimer complexes, it offers the possibility for the design of new ligands to allow water exchange, an important factor for MRI agents.

Despite the different position of the middle arm, the X-ray structures of the btt^{3-} isomers suggest that the N_4O cavity of the amine phenol ligand 1,1,4-btt^{3-} fits In^{3+} very well and that the 1,2,4-btt^{3-} cavity may be more appropriate for Ln^{3+} ions. Generally the better the fit between the metal ion and the cavity, the more stable is the resulting complex. The enlargement of the cavity can be achieved by changing the number of the donor atoms and carbons at the backbone. Further studies on ligands with different backbones, different cavities, and different water-solubilizing substituents are in progress.

Acknowledgment is made to the Natural Sciences and Engineering Research Council (NSERC) of Canada for a Postdoctoral Fellowship (S.L.) and an operating grant (C.O.) and to Professor J. Trotter for the very kind use of his crystallographic facilities.

Supplementary Material Available: Tables of ^{1}H and ^{13}C NMR and elemental analytical data and complete tables of crystallographic data, final atomic coordinates and equivalent isotropic thermal parameters, bond lengths, bond angles, anisotropic thermal parameters, hydrogen atom parameters, intermolecular contacts, and least-squares planes for the structures (113 pages). Ordering information is given on any current masthead page.

IC940514X

(46) Liu, S.; Rettig, S. J.; Orvig, C. *Inorg. Chem.* **1992**, *31*, 5400.